



## OPEN ACCESS

## EDITED BY

Shokrollah Elahi,  
University of Alberta, Canada

## REVIEWED BY

Thomas Tsutomu Murooka,  
University of Manitoba, Canada  
Elita Avota,  
Independent Researcher,  
Würzburg, Germany

## \*CORRESPONDENCE

Marek Widera  
marek.widera@kgu.de

## SPECIALTY SECTION

This article was submitted to  
Viral Immunology,  
a section of the journal  
Frontiers in Immunology

RECEIVED 04 May 2022

ACCEPTED 19 October 2022

PUBLISHED 15 November 2022

## CITATION

Sertznig H, Roesmann F, Wilhelm A,  
Heininger D, Bleekmann B, Elsner C,  
Santiago M, Schuhenn J, Karakoese Z,  
Benatzky Y, Snodgrass R, Esser S,  
Sutter K, Dittmer U and Widera M  
(2022) SRSF1 acts as an IFN-I-  
regulated cellular dependency  
factor decisively affecting HIV-1  
post-integration steps.  
*Front. Immunol.* 13:935800.  
doi: 10.3389/fimmu.2022.935800

## COPYRIGHT

© 2022 Sertznig, Roesmann, Wilhelm,  
Heininger, Bleekmann, Elsner, Santiago,  
Schuhenn, Karakoese, Benatzky,  
Snodgrass, Esser, Sutter, Dittmer and  
Widera. This is an open-access article  
distributed under the terms of the  
[Creative Commons Attribution License  
\(CC BY\)](https://creativecommons.org/licenses/by/4.0/). The use, distribution or  
reproduction in other forums is  
permitted, provided the original  
author(s) and the copyright owner(s)  
are credited and that the original  
publication in this journal is cited, in  
accordance with accepted academic  
practice. No use, distribution or  
reproduction is permitted which does  
not comply with these terms.

# SRSF1 acts as an IFN-I-regulated cellular dependency factor decisively affecting HIV-1 post-integration steps

Helene Sertznig<sup>1</sup>, Fabian Roesmann<sup>2</sup>, Alexander Wilhelm<sup>2</sup>,  
Delia Heininger<sup>2</sup>, Barbara Bleekmann<sup>1</sup>, Carina Elsner<sup>1</sup>,  
Mario Santiago<sup>3</sup>, Jonas Schuhenn<sup>1</sup>, Zehra Karakoese<sup>1</sup>,  
Yvonne Benatzky<sup>4</sup>, Ryan Snodgrass<sup>4</sup>, Stefan Esser<sup>5</sup>,  
Kathrin Sutter<sup>1</sup>, Ulf Dittmer<sup>1</sup> and Marek Widera<sup>1,2\*</sup>

<sup>1</sup>Institute for Virology, University Hospital Essen, University Duisburg-Essen, Essen, Germany,

<sup>2</sup>Institute for Medical Virology, University Hospital Frankfurt, Goethe University Frankfurt am Main, Frankfurt am Main, Germany, <sup>3</sup>Department of Medicine, University of Colorado Denver, Aurora, CO, United States, <sup>4</sup>Institute of Biochemistry I, Faculty of Medicine, Goethe-University Frankfurt am Main, Frankfurt, Germany, <sup>5</sup>Clinic of Dermatology, University Hospital, University of Duisburg-Essen, Essen, Germany

Efficient HIV-1 replication depends on balanced levels of host cell components including cellular splicing factors as the family of serine/arginine-rich splicing factors (SRSF, 1–10). Type I interferons (IFN-I) play a crucial role in the innate immunity against HIV-1 by inducing the expression of IFN-stimulated genes (ISGs) including potent host restriction factors. The less well known IFN-repressed genes (IRepGs) might additionally affect viral replication by downregulating host dependency factors that are essential for the viral life cycle; however, so far, the knowledge about IRepGs involved in HIV-1 infection is very limited. In this work, we could demonstrate that HIV-1 infection and the associated ISG induction correlated with low SRSF1 levels in intestinal lamina propria mononuclear cells (LPMCs) and peripheral blood mononuclear cells (PBMCs) during acute and chronic HIV-1 infection. In HIV-1-susceptible cell lines as well as primary monocyte-derived macrophages (MDMs), expression levels of SRSF1 were transiently repressed upon treatment with specific IFN $\alpha$  subtypes *in vitro*. Mechanically, 4sU labeling of newly transcribed mRNAs revealed that IFN-mediated SRSF1 repression is regulated on early RNA level. SRSF1 knockdown led to an increase in total viral RNA levels, but the relative proportion of the HIV-1 viral infectivity factor (Vif) coding transcripts, which is essential to counteract APOBEC3G-mediated host restriction, was significantly reduced. In the presence of high APOBEC3G levels, however, increased LTR activity upon SRSF1 knockdown facilitated the overall replication, despite

decreased *vif* mRNA levels. In contrast, SRSF1 overexpression significantly impaired HIV-1 post-integration steps including LTR transcription, alternative splice site usage, and virus particle production. Since balanced SRSF1 levels are crucial for efficient viral replication, our data highlight the so far undescribed role of SRSF1 acting as an IFN-modulated cellular dependency factor decisively regulating HIV-1 post-integration steps.

#### KEYWORDS

HIV-1, interferon, ISG (interferon stimulated genes), repressed genes, transcription, alternative splicing, SRSF1, SF2/ASF

## Introduction

Type I interferons (IFN-I), which, among others, include 12 individual IFN $\alpha$  subtypes and IFN $\beta$ , play a crucial role in the early innate immune defense against viral infections including HIV-1 (1, 2). After viral sensing *via* pattern recognition receptors (PRRs) like the Toll-like receptors (TLRs) or the cytosolic DNA sensor cyclic GMP-AMP synthase (cGAS), synthesis and secretion of IFN-I are induced (3–5). Binding of extracellular IFN-I to the IFN $\alpha$ / $\beta$ -receptor (IFNAR) induces signaling *via* the JAK/STAT-pathway and leads to the transcription of hundreds of IFN-stimulated genes (ISGs), such as host restriction factors or transcription factors establishing an antiviral state within the host and bystander cells (6–8). Among others, potent members of ISGs with anti-retroviral activity include ISG15 (IFN-stimulated gene 15) (9–11), APOBEC3G (apolipoprotein B mRNA editing enzyme and catalytic polypeptide-like 3G) (12, 13), tetherin (14, 15), Mx-2 (Myxovirus resistance-2) (16, 17), SAMHD1 (SAM domain and HD domain-containing protein 1) (18–20), and IFITM1-3 (Interferon-induced transmembrane protein 1-3) (21, 22). Despite a high sequence homology between IFN $\alpha$  subtypes and binding to the same receptor (IFNAR), all 12 individual IFN $\alpha$  subtypes were shown to exert different antiviral activities such as the induction of a distinct set of ISGs (23–25). While several IFN $\alpha$  subtypes were shown to elicit antiviral activity against human immunodeficiency virus type 1 (HIV-1), IFN $\alpha$ 14 has proven to be the most potent subtype (26, 27). However, IFN $\alpha$ 2, which is the sole subtype currently used in clinical treatments such as hepatitis B virus (HBV) infection (28), showed only limited antiviral activity against HIV-1.

In addition to the well-described induction of ISGs and other immunomodulatory functions, IFN-I also induces the repression of specific genes, termed IFN-repressed genes (IRepG) (29, 30). Several transcription factors were identified as IRepGs, suggesting a role in the restriction of cellular and viral gene

expression. Furthermore, distinct cellular factors including RNA-binding proteins (RBPs) that are crucial for viral replication could be identified as IRepGs (29, 31). Thus, their downregulation might represent a possible cellular defense mechanism limiting essential host dependency factors for HIV-1 replication.

Once integrated into the host cell genome, HIV-1 exploits the cellular transcription and RNA processing apparatus for viral gene expression (32, 33). The proviral DNA, which is under the transcriptional control of the LTR promoter, is transcribed as a full-length precursor mRNA (pre-mRNA) and undergoes excessive alternative splicing to extract the full genetic content of the short and compact genome (34–37). The usage of at least five splice donor sites (SD1 to SD4 including the alternative splice site SD2b) and multiple splice acceptor sites (SA1 to SA7) in various combinations allows the production of balanced levels of essential viral mRNAs. The recognition of these splice sites is regulated not only by their intrinsic strength but also by a complex network of splicing regulatory elements (SREs) located on the viral pre-mRNA (38, 39), both together referred to as the “splicing code” (40). Interaction of specific RBPs with SREs can, in a position-dependent manner, inhibit or promote the recognition and usage of a specific splice site (35, 37, 41, 42). These cellular splicing factors were defined as host dependency factors, which are essential for HIV-1 replication, but not lethal to the host cell upon gene silencing (43–47).

Serine/arginine-rich splicing factors (SRSFs) represent a large family of RBPs (48–51). Two main structural features are conserved among all SRSF proteins, the protein-interacting RS domain, which is rich in arginine and serine (RS) dipeptides, and the RNA recognition motif (RRM), which enables interactions with pre-mRNAs. SRSF proteins are generally characterized by their ability to interact with both RNA and protein structures simultaneously (52–54). SRSF protein activity and subcellular localization are mediated *via* post-translational modifications, such as phosphorylation (55), acetylation (56), or methylation

(57–59). Several members of this protein family have been shown to be crucial regulators of alternative splice site usage. While SRSF proteins promote binding of U1 snRNP or U2 snRNP to a 5'- or 3'-splice site and thus splice site recognition when binding to an SRE located in an exonic position (60–63), they repress splice site recognition when binding an SRE located in an intronic position, possibly due to steric hindrance (64–66). Furthermore, SRSF proteins were shown to regulate several other steps of gene expression, such as transcription (67, 68), nuclear mRNA export (69, 70), mRNA decay, or translation (71, 72). As the founding member of the SRSF protein family, serine/arginine-rich splicing factor 1 (SRSF1), formerly known as SRp30a or ASF/SF2 (73), was originally identified to promote spliceosomal assembly and pre-mRNA splicing in HeLa cells (74), as well as to regulate alternative splicing of the SV40 pre-mRNA in HEK293 cells (75). SRSF1 contains two RRM, providing the RNA-binding specificity, and a short RS domain (54). *In vivo* mapping identified the purine-rich sequence GGAGA as consensus motif of the SRSF1 binding site (76, 77).

SRSF1 has been described to play a crucial role in the regulation of gene expression and RNA processing of HIV-1 (78–81). Several SREs within the HIV-1 pre-mRNA are known targets of SRSF1, such as exonic splicing enhancer (ESE) M1/M2 (79), GAR-ESE (78), or ESE3 (80). Binding of SRSF1 to these *cis*-regulatory elements was shown to facilitate the recognition and usage of proximal splice sites. Furthermore, SRSF1 was shown to compete with Tat for a binding site within the TAR region on the LTR promoter, thereby interfering with the Tat-mediated HIV-1 LTR transactivation (82, 83). While high SRSF1 level resulted in enhanced Vpr, but reduced Tat1, Gag, and Env levels (84–86), low levels facilitated the expression of all viral mRNAs indicating a major impact on LTR transcription (84). Thus, SRSF1 represents a host dependency factor and key regulator for efficient HIV-1 RNA processing, enabling the emergence of the protein diversity necessary for efficient viral replication.

In this manuscript, we investigated whether the gene expression levels of SRSFs are influenced through HIV-1 infection and concomitant IFN-I stimulation. We observed a negative correlation between *ISG15* and *SRSF1* mRNA expression, particularly during acute HIV-1 infection. Furthermore, we identified *SRSF1* as a temporary IFN-regulated gene. Our findings suggest that balanced levels of SRSF1 are crucial for efficient HIV-1 replication, as in particular overexpression and knockdown resulted in severe impairments of HIV-1 post-integration steps at the level of LTR transcription, alternative splicing, or virus production. This work highlights the so far undescribed role of SRSF1 as IFN-regulated cellular effector molecule, decisively affecting HIV-1 LTR transcription and RNA processing, thereby contributing to the IFN-induced unfavorable cellular environment for HIV-1 replication.

## Results

### SRSF transcript levels are significantly lower in HIV-1-infected individuals

In a previous RNA-sequencing based study, we were able to demonstrate that compared to healthy donors, transcript levels of specific host restriction factors, such as tetherin, Mx-2, or APOBEC3G, were upregulated in intestinal lamina propria mononuclear cells (LPMCs) of HIV-1-infected treatment-naïve or antiretroviral therapy (ART)-treated individuals (87). To analyze whether host dependency factors including RBPs might also be altered upon HIV-1 infection, RNA-sequencing data were reanalyzed focusing on the gene expression of cellular splicing factors including *SRSF* family members. Significantly lower levels of mRNA transcripts were detected for *SRSF1* (1.8-fold) and *SRSF2* (1.4-fold) in HIV-1-infected treatment-naïve patients when compared to healthy individuals (Figure 1A; Supplementary Table 1). Furthermore, *SRSF3* (1.3-fold), *SRSF7* (1.4-fold), *SRSF8* (1.1-fold), and *SRSF10* (1.2-fold) transcript levels were also lower in this cohort, albeit without statistical significance (Figure 1A). In the cohort of HIV-1-infected and ART-treated patients, mRNA transcript levels of *SRSF2*, *SRSF7*, and *SRSF8* were comparable to the levels observed in the healthy control group, while *SRSF3* (1.2-fold) and *SRSF10* (1.1-fold) mRNA expression levels were still lower (Figure 1B). Of particular interest, transcript levels of *SRSF1* were significantly higher (1.2-fold) in HIV-1-infected ART-treated patients when compared to uninfected donors (Figure 1B). No significant difference in transcript levels were observed upon HIV-1 infection, either treatment-naïve or under ART treatment, for *SRSF4*, *SRSF5*, *SRSF6*, and *SRSF11* when compared to healthy individuals (Figures 1A, B). In all patient groups, *SRSF9* and *SRSF12* transcript levels were only marginally above the limit of detection (Figures 1A, B). Since, concomitant to the elevated ISG profile (87), mRNA transcript levels of several *SRSFs* were lower in HIV-1-infected individuals, a possible correlation with interferon signaling and chronic inflammation was further investigated. Since SRSF1 was the most significant differentially expressed gene of the SRSF family in LPMCs of HIV-1-positive patients and was also previously described to be crucially involved in HIV-1 post-integration steps (78–81), the expression profile of SRSF1 was analyzed in peripheral blood mononuclear cells (PBMCs) of another cohort of HIV-1-infected individuals at various infection stages (88). For this purpose, PBMCs were isolated from HIV-1-positive individuals during acute infection (Fiebig I–V), chronic infection (Fiebig VI), or chronic infection phase under ART treatment as well as from HIV-1-negative healthy donors. Total cellular RNA was isolated and subjected to RT-qPCR analysis. To evaluate whether the patient cohort was representative, *ISG15* mRNA expression

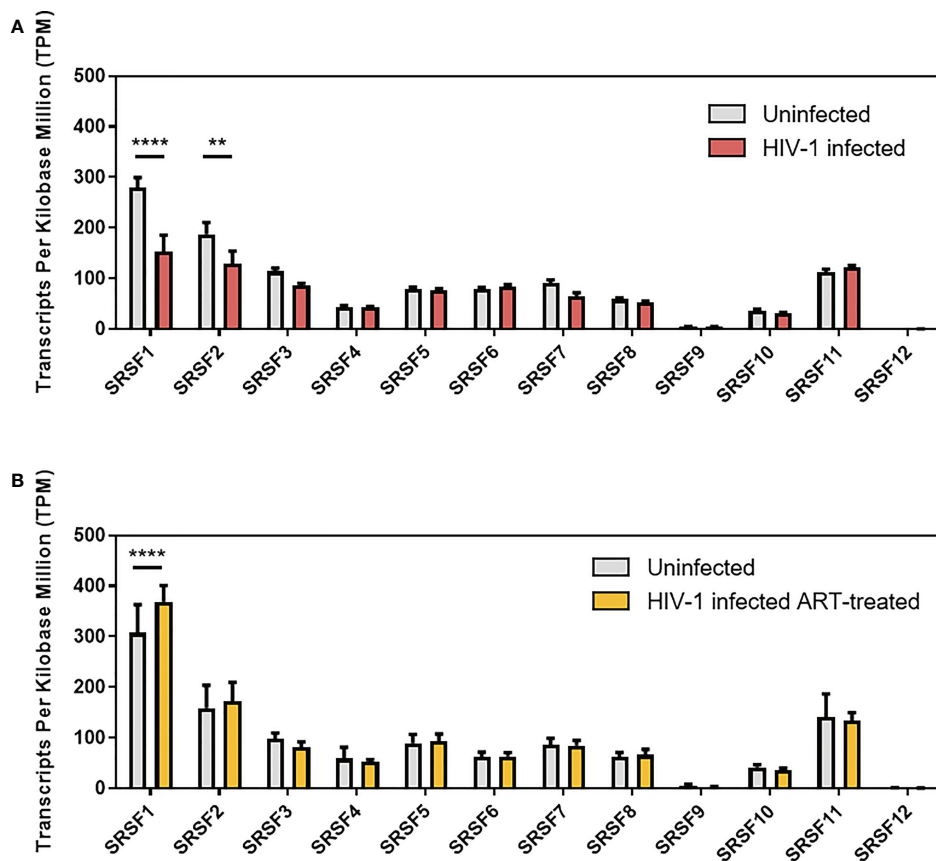


FIGURE 1

Gene expression levels of *SRSFs* in treatment-naïve or ART-treated HIV-1-infected individuals. Transcript levels of *SRSF* genes were measured in lamina propria mononuclear cells (LPMCs) from the gut using RNA-sequencing analysis (Supplementary Table 1). Comparison of transcript levels from (A) treatment-naïve HIV-1-infected and healthy individuals and (B) ART-treated HIV-1-infected and healthy individuals. TPM are depicted as mean (+ SD) for (A) 19 HIV-1-infected and 13 uninfected individuals and (B) 14 ART-treated and 11 uninfected individuals. Groups were compared with two-way ANOVA with Bonferroni *post-hoc* test (\*\* $p < 0.01$ , and \*\*\*\* $p < 0.0001$ ).

was determined as a surrogate marker for IFN signature, since it was previously demonstrated that ISG expression levels are induced upon HIV-1 infection in PBMCs (23). When compared to healthy individuals, *ISG15* mRNA expression levels were 5.6- and 7.3-fold higher in acutely and chronically HIV-1-infected patients, respectively, while ART-treated patients only had 2.2-fold higher *ISG15* mRNA levels (Figure 2A). The virus-induced IFN signature was found to be proportional to the plasma viral load upon both acute and chronic HIV-1 infection (Figure 2B). Next, we performed a specific RT-qPCR analysis to investigate whether the *SRSF1* repression might correlate with ISG induction in HIV-1-infected patients. For acutely and chronically HIV-1-infected patients, 2- and 2.6-fold lower levels of *SRSF1* mRNA, respectively, were detected in contrast to healthy donors (Figure 2C). Upon ART treatment, *SRSF1* mRNA expression levels were 2.6-fold lower when compared to uninfected individuals (Figure 2C). While *SRSF1* mRNA levels were lower

in the majority of the samples derived from acutely and chronically HIV-1-infected treatment-naïve patients in contrast to the healthy control group, *SRSF1* expression levels were increased in some patients (Figure 2C). Since most individuals with higher levels of *SRSF1* mRNA also had no or only marginally induced levels of *ISG15* mRNA, they were defined as low responders and excluded from statistical analysis (marked in light pink). No significant correlation was detected between the repression of *SRSF1* mRNA and the plasma viral load of acutely and chronically HIV-1-infected patients (Figure 2D). Generally, high levels of *ISG15* mRNA expression were concomitant with a strong repression of *SRSF1* mRNA levels in single individuals (Figure 2E). The determination of Pearson correlation coefficients revealed a negative correlation between *ISG15* and *SRSF1* mRNA expression upon acute HIV-1 infection (Figure 2F). No direct correlation between ISG induction and *SRSF1* repression could be found for the group of chronically HIV-1-infected individuals, which generally



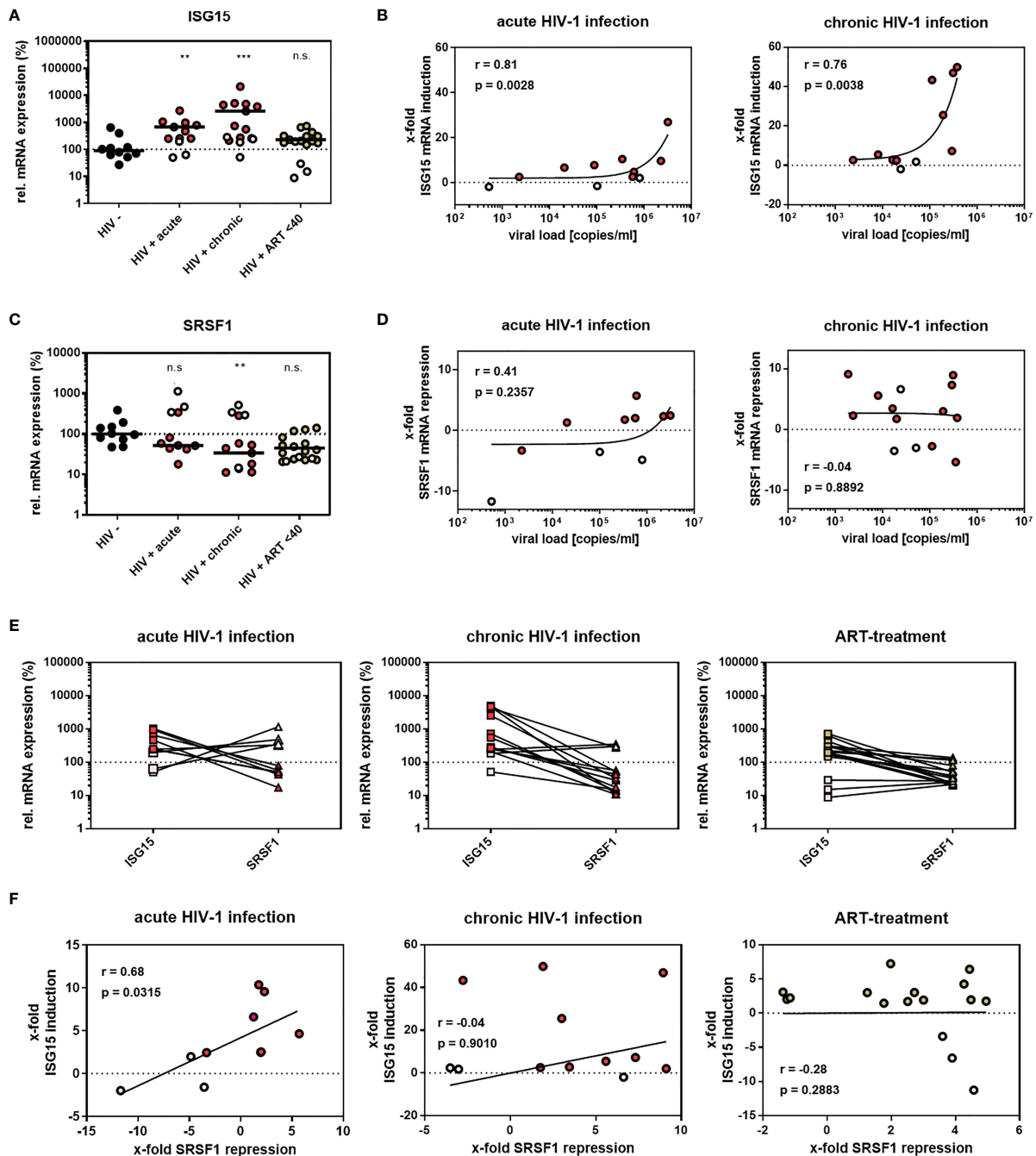


FIGURE 2

*SRSF1* and *ISG15* expression levels inversely correlate upon HIV-1 infection. (A, C) RT-qPCR determined the relative mRNA expression levels of (A) *ISG15* and (C) *SRSF1* in PBMCs from acutely and chronically HIV-1-infected patients, either naïve or under ART treatment as well as healthy donors. ACTB was used for normalization. Kruskal–Wallis test with the Dunn’s *post-hoc* multiple comparisons test was used to determine whether the difference between the group of samples reached the level of statistical significance (\*\* $p < 0.01$ , \*\*\* $p < 0.001$  and ns, not significant). (B, D) Correlation between plasma viral load of HIV-1-infected individuals and *ISG15* and *SRSF1* mRNA expression. RT-qPCR analysis was performed to determine *ISG15* and *SRSF1* mRNA expression. Pearson correlation was calculated between plasma viral load and (B) *ISG15* or (D) *SRSF1* expression for acutely and chronically HIV-1-infected patients. Pearson correlation coefficient ( $r$ ) and  $p$ -value ( $p$ ) are indicated. (E) Comparison of relative *ISG15* and *SRSF1* mRNA levels for individual patients. (F) Calculated correlation between x-fold repression of *SRSF1* mRNA levels and x-fold induction of *ISG15* mRNA levels for all patient groups. Pearson correlation coefficient ( $r$ ) and  $p$ -value ( $p$ ) are indicated. Data points from healthy donors were depicted in black, while data points from treatment-naïve HIV-1-infected individuals were shown in red. ART-treated patients are colored in green. Patients with no or low *ISG15* mRNA induction upon HIV-1 infection were considered as low responders without IFN signature and were thus excluded from statistical analysis (light gray). This patient cohort included 10 uninfected donors, 8 acutely HIV-1-infected patients, 11 chronically HIV-1-infected patients, and 13 HIV-1-infected patients under ART treatment.

represent a heterogeneous cohort due to unmatched infection phases, comorbidities, and other factors (89, 90). Consistent with the previous data, we did not observe any correlation between *ISG15* and *SRSF1* expression in the group of ART-treated individuals (Figure 2F).

In conclusion, since we revealed a possible link between the stimulation of ISGs and *SRSF1* repression, *SRSF1* might potentially represent an IRepG as part of the immune response to HIV-1.

## The degree of *SRSF1* repression is IFN $\alpha$ subtype dependent

We previously showed that IFN $\alpha$  subtypes exert distinct antiviral activities upon HIV-1 infection and that their antiviral potential correlates with the induction of ISGs including host restriction factors (26, 27). To assess whether the observed correlation between ISG induction and *SRSF1* repression in the early immune response upon HIV-1 infection was induced by IFN signaling, the effect of IFN $\alpha$  subtypes ( $\alpha$ 1,  $\alpha$ 2,  $\alpha$ 4,  $\alpha$ 5,  $\alpha$ 6,  $\alpha$ 7,  $\alpha$ 10,  $\alpha$ 14,  $\alpha$ 16,  $\alpha$ 17, and  $\alpha$ 21) on the mRNA expression levels of *ISG15* and *SRSF1* was analyzed.

Using a reporter cell line (RPE-ISRE luc) that harbors the firefly luciferase gene under the control of the IFN-inducible ISRE promoter, we evaluated the biological activity of the IFN $\alpha$  subtypes confirming a strong activity except for IFN $\alpha$ 1, IFN $\alpha$ 7, and IFN $\alpha$ 21 (Supplementary Figure 1). Next, THP-1 monocytic cells were differentiated into macrophage-like cells using phorbol 12-myristate 13-acetate (PMA) and treated with IFN $\alpha$  subtypes. In general, the intensity of *ISG15* induction reflected the intensity of the luminescent signal in the reporter cells (Figure 3A and Supplementary Figure 1). Subtypes IFN $\alpha$ 2 (124.7-fold), IFN $\alpha$ 4 (223.4-fold), IFN $\alpha$ 6 (106.2-fold), and IFN $\alpha$ 14 (94.5-fold) induced the strongest *ISG15* mRNA expression when compared to the unstimulated control (Figure 3A). Treatment with IFN $\alpha$ 5 (32.3-fold), IFN $\alpha$ 10 (62.1-fold), IFN $\alpha$ 16 (17.1-fold), IFN $\alpha$ 17 (47.0-fold), and IFN $\alpha$ 21 (18.5-fold) led to a moderate but not significant *ISG15* increase, while treatment with IFN $\alpha$ 1 (5.4-fold) and IFN $\alpha$ 7 (3.4-fold) did not significantly alter *ISG15* mRNA expression (Figure 3A). These data were in accordance with previous findings, which described the induction of other ISGs such as Mx2, TRIM22, and APOBEC3G (Supplementary Figure 2) upon stimulation with specific IFN $\alpha$  subtypes (23).

The strongest repression in *SRSF1* mRNA expression was observed for subtypes IFN $\alpha$ 10 (4.2-fold) and IFN $\alpha$ 14 (12.5-fold), while subtypes IFN $\alpha$ 4 (2.3-fold), IFN $\alpha$ 6 (2.3-fold), IFN $\alpha$ 7 (2.5-fold), IFN $\alpha$ 17 (2.7-fold), and IFN $\alpha$ 21 (2.1-fold) induced a moderate but significant *SRSF1* mRNA repression (Figure 3B). Changes in *SRSF1* mRNA expression observed upon stimulation with subtypes IFN $\alpha$ 1 (1.3-fold), IFN $\alpha$ 2 (1.5-fold), IFN $\alpha$ 5 (1.2-fold), and IFN $\alpha$ 16 (1.3-fold) were not significant (Figure 3B).

Remarkably, not all subtypes induced an inverse correlation between *ISG15* induction and *SRSF1* repression. A strong induction in *ISG15* mRNA expression was observed upon treatment with IFN $\alpha$ 2, IFN $\alpha$ 4, and IFN $\alpha$ 6; however, these subtypes only induced a weak repression in *SRSF1* mRNA. IFN $\alpha$ 14 induced a disproportionately strong repression in *SRSF1* mRNA levels compared to the stimulation of *ISG15* mRNA expression.

In conclusion, in agreement with previous work (7, 25, 91, 92), the degree of ISG induction was IFN $\alpha$  subtype dependent, suggesting distinct antiviral activities. Generally, all IFN $\alpha$  subtypes induced a repression of *SRSF1* mRNA levels, albeit to a highly varying extent, with IFN $\alpha$ 10 and IFN $\alpha$ 14 being the most potent. These results substantiate the assumption of *SRSF1* representing an IRepG.

In our further studies, we included the subtypes IFN $\alpha$ 2 and IFN $\alpha$ 14 as IFN $\alpha$ 14 was shown to be the most potent subtype against HIV-1 (27) and induced the strongest downregulation of *SRSF1* mRNA levels (Figure 3B), while IFN $\alpha$ 2 is the sole IFN $\alpha$  subtype currently in clinical use for the treatment of other viral infections such as HBV (28).

To assess whether the downregulation of *SRSF1* is a direct effect of IFN treatment, we added Ruxolitinib, which is a Janus kinase inhibitor (JAK1 and JAK2) and thus blocks the IFN signaling pathway (93). At 4 and 8 h post-treatment, the addition of Ruxolitinib resulted in significantly reduced *ISG15* expression, when compared to unblocked administration of IFN $\alpha$ 14 (Figure 3C).

Since *ISG15* was described to additionally be modulated by a non-Jak1/2 dependent pathway, we monitored the expression of *IFITM1* as an additional Jak1/2-dependent ISG. In agreement with previous studies (94), Ruxolitinib significantly reduced *IFITM1* mRNA expression at 4 to 48 h post-treatment, albeit only statistically significant at 4, 8, and 48 h (Figure 3D). However, complete inhibition of both ISGs could not be observed, potentially due to JAK1/2-independent pathways. This observation was in agreement with previous studies showing a strong *ISG15* induction by viral infections (9). *SRSF1* expression was significantly higher upon treatment with Ruxolitinib after 12 and 24 h of IFN $\alpha$ 14 treatment (Figure 3E) while no reduction of *SRSF1* mRNA expression was observed in the presence of Ruxolitinib. These results confirm the correlation in the induction of IFN-stimulated genes and *SRSF1* repression.

## *SRSF1* is an IFN-regulated gene in HIV-1 target cells

To further assess the suggested role of *SRSF1* acting as IRepG, we examined *SRSF1* expression levels in HIV-1 target cells upon IFN stimulation in a time-course experiment. In differentiated THP-1 macrophages, we observed a strong 100- to 1,000-fold induction of *ISG15* mRNA expression levels

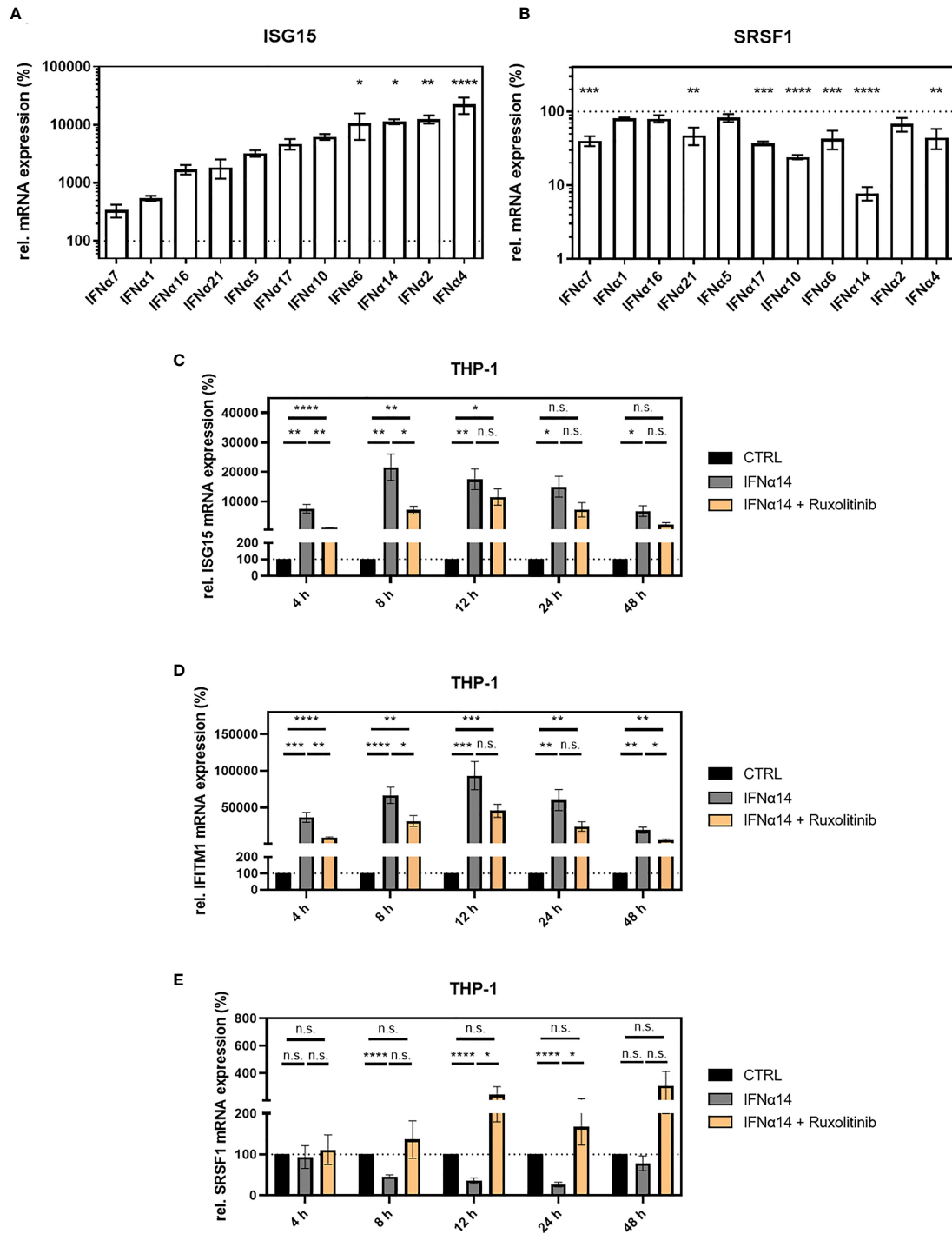


FIGURE 3

*SRSF1* expression upon stimulation with IFN $\alpha$  subtypes. Differentiated THP-1 cells were treated with the indicated IFN subtype (10 ng/ml). Twenty-four hours post-treatment, cells were harvested, and RNA was isolated and subjected to RT-qPCR for measurement of relative (A) *ISG15* and (B) *SRSF1* mRNA expression levels. Statistical significance was analyzed performing one-way ANOVA with Dunnett *post-hoc* test (\* $p < 0.05$ , \*\* $p < 0.01$ , \*\*\* $p < 0.001$ , and \*\*\*\* $p < 0.0001$ ). Mean ( $\pm$  SEM) of  $n = 3$  biological replicates is depicted. (C–E) Differentiated THP-1 cells were treated with 1  $\mu$ M Ruxolitinib or DMSO as mock control 1 h before infection using NL4-3 AD8 (1 MOI). Sixteen hours post-infection, cells were washed with PBS and treated with media containing PBS or IFN $\alpha$ 14, and either Ruxolitinib or DMSO. At the indicated time points, wells were rinsed with PBS, and cells were subjected to RNA isolation and RT-qPCR analysis to monitor mRNA expression levels of (C) *ISG15*, (D) *IFITM1*, and (E) *SRSF1*. Groups were compared with two-way repeated-measures ANOVA with Tukey's *post-hoc* test. ns is not significant.

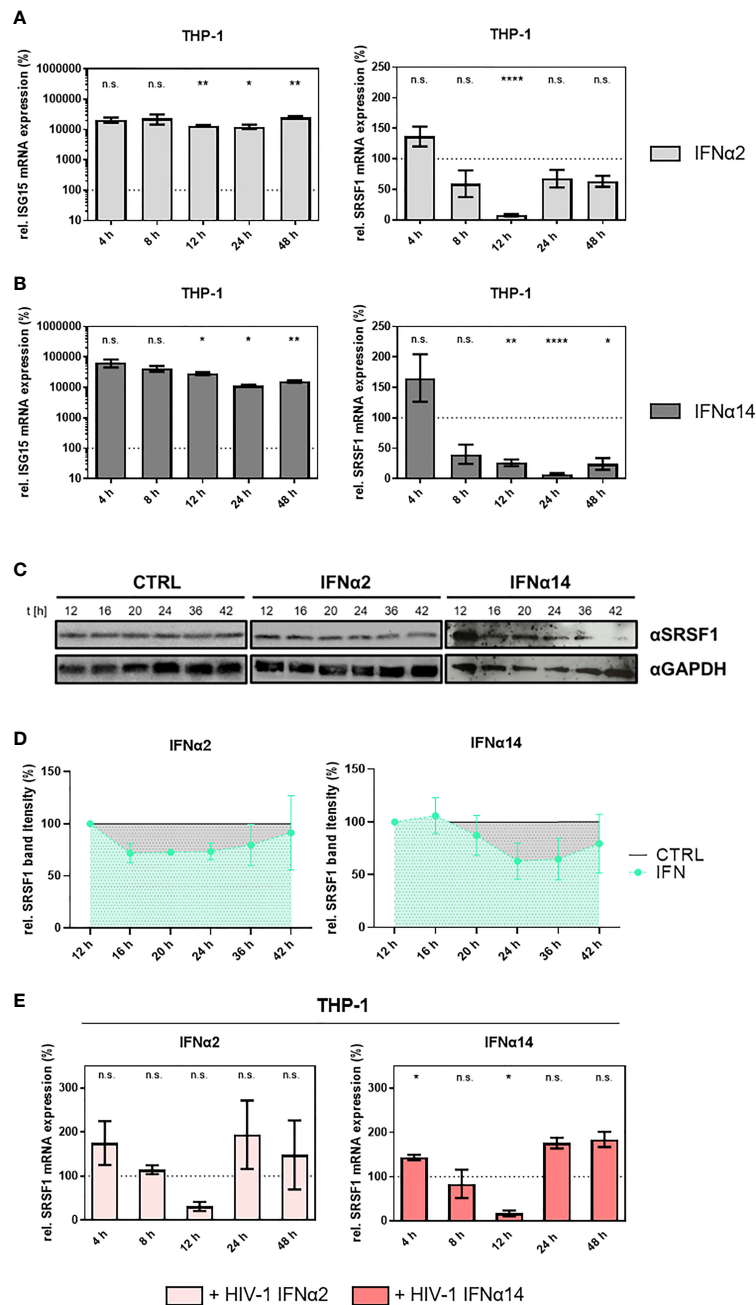


FIGURE 4

*SRSF1* mRNA and protein levels are differentially regulated upon stimulation of macrophages with IFNα2 or IFNα14. Differentiated THP-1 macrophages were treated with IFNα2 (light gray) or IFNα14 (dark gray) (10 ng/ml) over a period of 48 h before cells were harvested and RNA was isolated. Relative mRNA expression levels were measured via RT-qPCR analysis. (A, B) Relative mRNA expression levels of *ISG15* and *SRSF1* upon stimulation with (A) IFNα2 or (B) IFNα14 in THP-1 cells. Mixed-effects analyses followed by Dunnett's *post-hoc* test were used to compare differences between groups at different time points (\* $p < 0.05$ , \*\* $p < 0.01$ , \*\*\* $p < 0.0001$  and ns, not significant). (C) Differentiated THP-1 macrophages were treated with IFNα2 or IFNα14 (10 ng/ml) for the indicated amount of time before cells were harvested and proteins were isolated. Proteins were separated by SDS-PAGE, blotted, and analyzed with an antibody specific to SRSF1. A representative Western blot is shown using GAPDH as a loading control. (D) Quantification of multiple Western blots ( $n = 4$  for IFNα14,  $n = 3$  for IFNα2). Total protein amount was stained using Trichloroethanol and used as loading control. Band intensity was measured using ImageJ software. Mixed-effects analyses followed by Dunnett's *post-hoc* test. (E) Differentiated THP-1 macrophages were infected with the R5-tropic NL4-3 (AD8) (95) at an MOI of 1. Sixteen hours post-infection, cells were treated with the indicated IFN subtype (10 ng/ml) over a period of 48 h. Cells were harvested at the indicated time points, and RNA was isolated and subjected to RT-qPCR. Relative mRNA expression levels of *SRSF1* in THP-1 cells after treatment with IFNα2 or IFNα14 as indicated. GAPDH was used as a house-keeping gene for normalization. Mixed-effects analyses followed by Dunnett's *post-hoc* test were used to determine whether the difference between the group of samples reached the level of statistical significance (\* $p < 0.05$ , \*\* $p < 0.01$ , \*\*\* $p < 0.001$  and \*\*\*\* $p < 0.0001$ ). Mean ( $\pm$  SEM) of  $n = 4$  biological replicates is shown.

remaining high up to 48 h post-stimulation with IFN $\alpha$ 2 and IFN $\alpha$ 14 (Figures 4A, B, left panel). Treatment with IFN $\alpha$ 2 resulted in a 13-fold and highly significant downregulation of *SRSF1* after 12 h while expression levels were restored (less than twofold) 24–48 h post-treatment (Figure 4A, right panel). Treatment with IFN $\alpha$ 14 also resulted in a significant 13-fold downregulation of *SRSF1* after 24 h, but for this subtype, a longer-lasting effect with a still 6-fold significant downregulation was observed after 48 h (Figure 4B, right panel). Overall, IFN $\alpha$ 14 induced a stronger and more continuous repression than IFN $\alpha$ 2. Interestingly, stimulation with both IFN $\alpha$ 2 and IFN $\alpha$ 14 induced an initial increase of 2.2- and 1.7-fold, respectively, in *SRSF1* mRNA expression 4 h post-treatment, albeit not statistically significant (Figures 4A, B, right panel).

To further analyze whether the IFN-induced reduction of *SRSF1* could also be observed on protein level, we performed Western blot analysis of IFN-treated THP-1 cells. Both stimulation with IFN $\alpha$ 2 and IFN $\alpha$ 14 resulted in a time-dependent decrease in *SRSF1* protein levels (Figures 4C, D). While treatment with IFN $\alpha$ 2 only led to a weak repression, treatment with IFN $\alpha$ 14 resulted in a more pronounced and longer-lasting downregulation of *SRSF1* protein levels (Figure 4C), which was in accordance with the mRNA expression levels (Figures 3A and 4A, B, right panel). When compared to the mRNA levels, *SRSF1* protein levels decreased with a delay of 8–12 h, which might be explained by the half-life of persisting mRNA and protein levels. In agreement with the previous RNA data, the reduction in protein levels was observed earlier for IFN $\alpha$ 2- than for IFN $\alpha$ 14-treated cells. After the initial reduction, the protein levels were restored almost to initial levels at 42 h post-stimulation. Remarkably, IFN $\alpha$ 14-treated cells tend to have a slow and more pronounced decrease in *SRSF1* levels. However, this reduction was not significant due to the variability of the Western blotting procedure (Figure 4D). The protein amount continuously declined 16 h post-IFN $\alpha$ 14 induction and was restored up to 60% of the initial level 42 h post-stimulation.

Next, we were interested whether a previous HIV-1 infection would affect the IFN-mediated time-dependent regulation of *SRSF1*. Therefore, we infected THP-1 macrophages with the R5-tropic HIV-1 laboratory strain NL4-3 AD8 16 h before stimulation with IFN $\alpha$ 2 or IFN $\alpha$ 14. This time point was specifically chosen to focus on HIV-1 post-integration steps, as the integration of the viral genome into the host cell genome is mostly completed (96). In infected THP-1 macrophages, treatment with IFN $\alpha$ 2 and IFN $\alpha$ 14 induced a comparable profile of *SRSF1* mRNA expression (Figure 4E). An initial upregulation, which was only significant for IFN $\alpha$ 14, was observed after 4 h by 1.7- and 1.4-fold for IFN $\alpha$ 2 and IFN $\alpha$ 14, respectively. Treatment with IFN $\alpha$ 2 resulted in a nonsignificant ( $p = 0.0522$ ) 3.3-fold decrease in *SRSF1* mRNA levels after 12 h in HIV-1-infected cells (Figure 4E). Stimulation with IFN $\alpha$ 14 resulted in a significant ( $p = 0.0139$ ) 5.9-fold reduced *SRSF1*

expression after 12 h, which was restored after 24 and 48 h (Figure 4E).

While a 13-fold repression was observed in uninfected cells upon stimulation with IFN $\alpha$ 2 and IFN $\alpha$ 14 after 12 and 24 h, respectively, stimulation of HIV-1-infected cells only resulted in a 3.3-fold (IFN $\alpha$ 2) and 5.9-fold (IFN $\alpha$ 14) decrease in *SRSF1* mRNA levels 12 h post-treatment. Thus, the magnitude of repression was stronger in uninfected cells when compared to HIV-1-infected cells. While the *SRSF1* expression profile upon stimulation with IFN $\alpha$ 2 and IFN $\alpha$ 14 was different in uninfected cells, no large discrepancies were observed upon treatment of HIV-1-infected cells with both subtypes. Contrary to uninfected cells, *SRSF1* mRNA expression was restored already 24 h post-stimulation of HIV-1-infected cells with IFN $\alpha$ 14.

Since viral proteins were shown to modulate the expression of cellular genes (97–101), we next overexpressed a panel of HIV-1 accessory proteins in HEK293T cells. Consistent with previous literature (97, 98), we confirmed that the viral protein Vpr was able to significantly increase ISG15 expression (Supplementary Figure 3). Further analysis with a full-length viral genome and a Vpr-deficient derivative confirmed the significant involvement of Vpr in an infectious context. Since an inverse correlation between ISG induction and *SRSF1* repression has been observed, Vpr could potentially be directly involved in the downregulation of *SRSF1* observed upon HIV-1 infection.

To assess, whether these findings could be transferred to primary human cells, we analyzed gene expression of *SRSF1* after stimulation of primary human monocyte-derived macrophages (MDMs) with IFN $\alpha$ 14. A strong 50- to 500-fold induction was observed for *ISG15* mRNA expression levels in all three tested donors (Figure 5A, left panel). Concomitantly, a time-dependent repression of *SRSF1* mRNA was detected with a 1.5-fold (donor 3), 2.8-fold (donor 2), and 4.1-fold (donor 1) downregulation after 8 h (Figure 5A, right panel), thus supporting a potential role of *SRSF1* as IRepG in primary human macrophages. Of note, the IFN $\alpha$ 14-induced downregulation of *SRSF1* mRNA levels was less pronounced in MDMs than in THP-1 macrophages. While IFN $\alpha$ 14 induced a long-lasting and strong repression of *SRSF1* mRNA expression in THP-1 macrophages, *SRSF1* mRNA levels in MDMs were comparable to the untreated control already after 12–24 h.

To analyze whether the downregulation of *SRSF1* was IFN-I specific, we included IFN $\gamma$  as the sole member of the type II IFN family (IFN-II) (102, 103). Since IFN $\gamma$  binds to the IFN $\gamma$  receptor (IFNGR) and activates a distinct signaling pathway than IFN-I (8, 102, 104), IFN-regulatory factor 1 (IRF1) was chosen as a control of IFN-II-specific activation of the IFN $\gamma$  activation site (GAS) regulated promotor (105, 106). Stimulation of THP-1 macrophages with IFN $\gamma$  led to a strong 50- to 100-fold induction of *IRF1* mRNA 4–24 h after stimulation. After 48 h, only a remaining ninefold induction in *IRF1* mRNA expression was



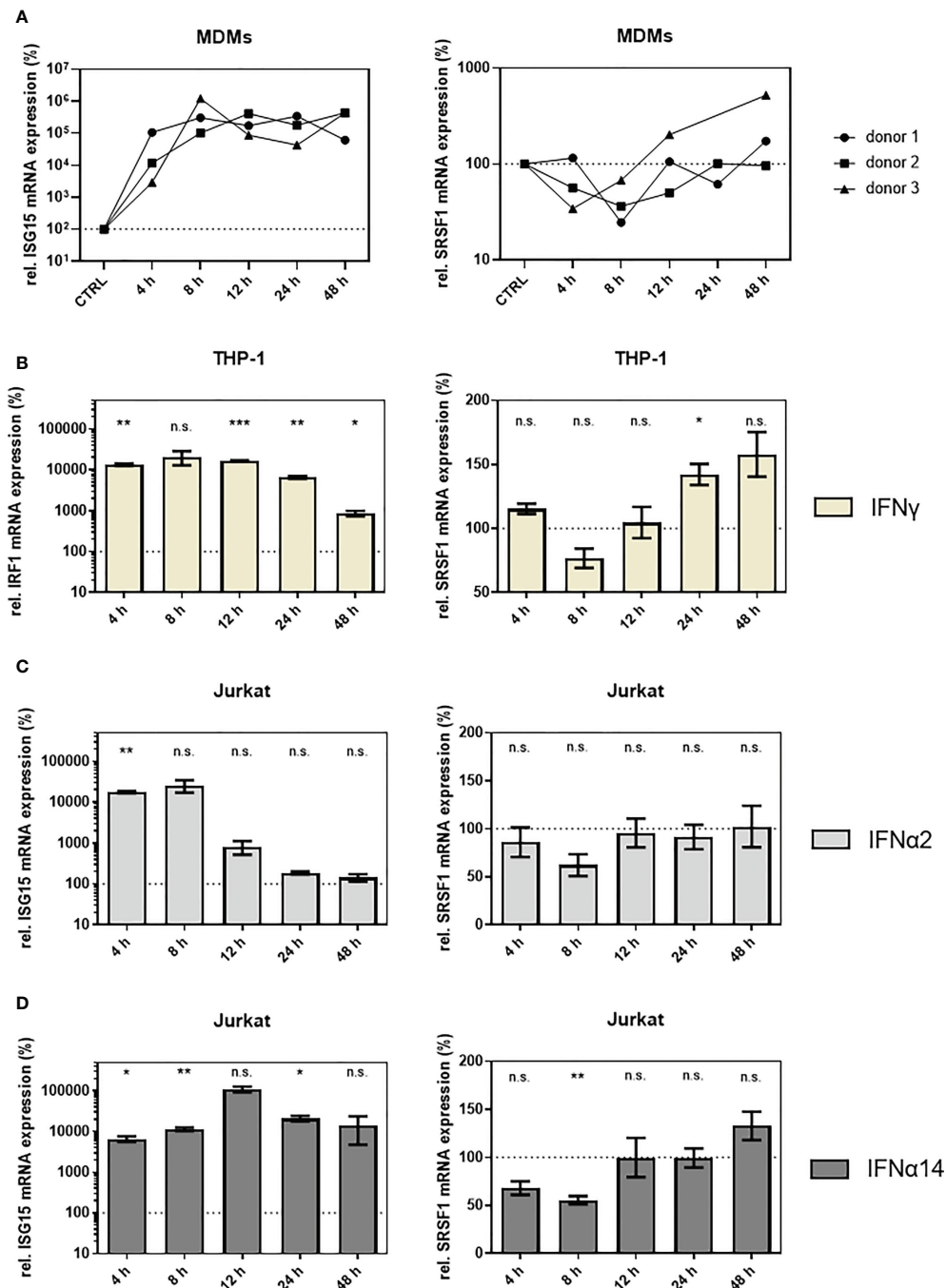


FIGURE 5

*SRSF1* mRNA levels are differentially regulated upon treatment of HIV-1 target cells with IFNs. **(A)** Monocyte-derived macrophages (MDMs) were treated for 48 h with 10 ng/ml of IFN $\alpha$ 14. After harvesting the cells, RNA was extracted and subjected to RT-qPCR. Relative mRNA expression levels of *ISG15* and *SRSF1* are shown. Expression levels were normalized to GAPDH. Time point of 24 h only includes two biological replicates. **(B)** Differentiated THP-1 cells were stimulated with IFN $\gamma$  (10 ng/ml) for 48 h before cells were harvested and RNA was isolated. Relative mRNA expression levels of *IRF1* and *SRSF1* were measured via RT-qPCR. GAPDH was used as a house-keeping gene for normalization. Mixed-effects analysis followed by Dunnett's *post-hoc* test was conducted to determine whether the difference between the group of samples reached the level of statistical significance (\* $p$  < 0.05, \*\* $p$  < 0.01, \*\*\* $p$  < 0.001, and ns, not significant). Mean ( $\pm$  SEM) of  $n$  = 4 biological replicates is shown. **(C, D)** Relative mRNA expression levels of *ISG15* and *SRSF1* upon stimulation with **(C)** IFN $\alpha$ 2 or **(D)** IFN $\alpha$ 14 in Jurkat cells. ACTB was used as a house-keeping gene for normalization. Mixed-effects analysis with Dunnett's *post-hoc* test was performed to determine whether the difference between the group of samples reached the level of statistical significance (\* $p$  < 0.05, \*\* $p$  < 0.01, \*\*\* $p$  < 0.001, and ns, not significant). Mean ( $\pm$  SEM) of  $n$  = 4 biological replicates is shown.

observed (Figure 5B, left panel). IFN $\gamma$  treatment only induced a weak and nonsignificant 1.3-fold downregulation in *SRSF1* mRNA expression levels after 8 h. Remarkably, 12–48 h post-stimulation, a time-dependent increase in *SRSF1* mRNA was observed with significantly elevated levels after 24 h (1.4-fold) (Figure 5B, right panel). Hence, the IFN-mediated regulation of *SRSF1* mRNA expression seems to also involve IFN-II signaling.

In Jurkat T cells, treatment with IFN $\alpha$ 2 led to a significant 100-fold induction in *ISG15* mRNA expression levels after 4 h, while 12-h post-stimulation *ISG15* levels drastically dropped to the levels comparable to PBS-treated control cells (Figure 5C, left panel). Treatment with IFN $\alpha$ 14 resulted in a continuous (24 h) 100- to 1,000-fold significant induction of *ISG15* mRNA expression levels (Figure 5D, left panel). Treatment with IFN $\alpha$ 14 resulted in twofold ( $p = 0.0057$ ) repression after 8 h (Figure 5D, right panel). *SRSF1* mRNA expression levels were restored 12 h post-stimulation (Figure 5D, right panel).

Thus, a time-dependent downregulation in *SRSF1* mRNA levels was observed in HIV-1 target cells upon treatment with IFN $\alpha$ 14, suggesting a potential role of *SRSF1* as an IRepG. Since the repression of *SRSF1* mRNA expression was much more pronounced in THP-1 macrophages than in Jurkat T cells, a cell-type-specific effect was suggested.

## Deregulation of SRSF1 expression occurs on RNA level

*SRSF1* was identified as an IFN-regulated gene in HIV-1 target cells; however, the mechanistic mode of action was still unknown. To assess whether the IFN-mediated deregulation of *SRSF1* mRNA expression occurred on the transcriptional level, we used the method of 4-thiouridine (4sU)-tagging (30, 107–110). This method allows the metabolic labeling of freshly

transcribed RNA using 4sU, enabling the subsequent purification and separation of newly synthesized RNA from untagged pre-existing RNA. THP-1 macrophages were treated with IFN $\alpha$ 14 for 4, 8, or 24 h and 4sU was added 30 min prior to cell harvest. Following the biotinylation of the incorporated 4sU, the freshly transcribed RNA was separated from the unlabeled RNA using Streptavidin-coated magnetic beads. Changes in transcription rates were measured *via* RT-qPCR. Comparison to the untreated control stimulation with IFN $\alpha$ 14 resulted in a significant increase in *ISG15* mRNA expression after 4 and 24 h (319- and 352-fold), respectively (Figure 6A). Remarkably, a 33-fold, but nonsignificant, increase in *SRSF1* mRNA expression was observed 4 h post-treatment (Figure 6B). A significant 2.5-fold reduction in *SRSF1* mRNA expression was observed after 8 h, which was still significantly reduced by 2.9-fold after 24 h (Figure 6B).

These data indicate that the IFN-mediated regulation of *SRSF1* likely occurs on the transcriptional level. The expression profile of *SRSF1* analyzing 4sU-labeled and freshly transcribed RNA was in accordance with the expression profile of *SRSF1* analyzing total RNA (Figure 4B, right panel). Both data sets revealed a multi-phasic pattern with an early increase in mRNA expression followed by a strong downregulation.

## Knockdown of SRSF1 levels affect HIV-1 post-integration steps

*SRSF1* has been described as a crucial regulator in HIV-1 post-integration steps. In addition to *SRSF1* regulating alternative splice site usage *via* targeting several binding sites on the viral pre-mRNA (78, 81), *SRSF1* was also described to compete with binding of HIV-1 Tat to a sequence within the TAR region, thereby impeding HIV-1 LTR activity (83).

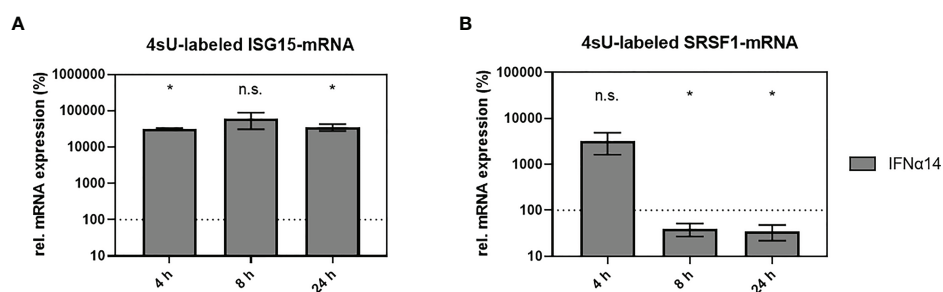


FIGURE 6

IFN $\alpha$ 14-mediated changes in newly transcribed *SRSF1* mRNA. (A, B) THP-1 macrophages were stimulated with IFN $\alpha$ 14 (10 ng/ml). 4-Thiouridine (4sU) was added 30 min before harvesting the cells at the indicated time points in order to label newly synthesized RNA. After separation and isolation of the freshly synthesized RNA, RT-qPCR was performed to measure relative mRNA expression levels of (A) *ISG15* and (B) *SRSF1*. GAPDH was used as a house-keeping gene for normalization. Statistical significance compared to untreated control was determined using unpaired two-sided Welch's t-test. Asterisks indicated  $p$ -values as  $*p < 0.05$  and ns, not significant. Mean ( $\pm$  SEM) of  $n = 3$  biological replicates is shown (except for 4 h, where  $n = 2$ ).

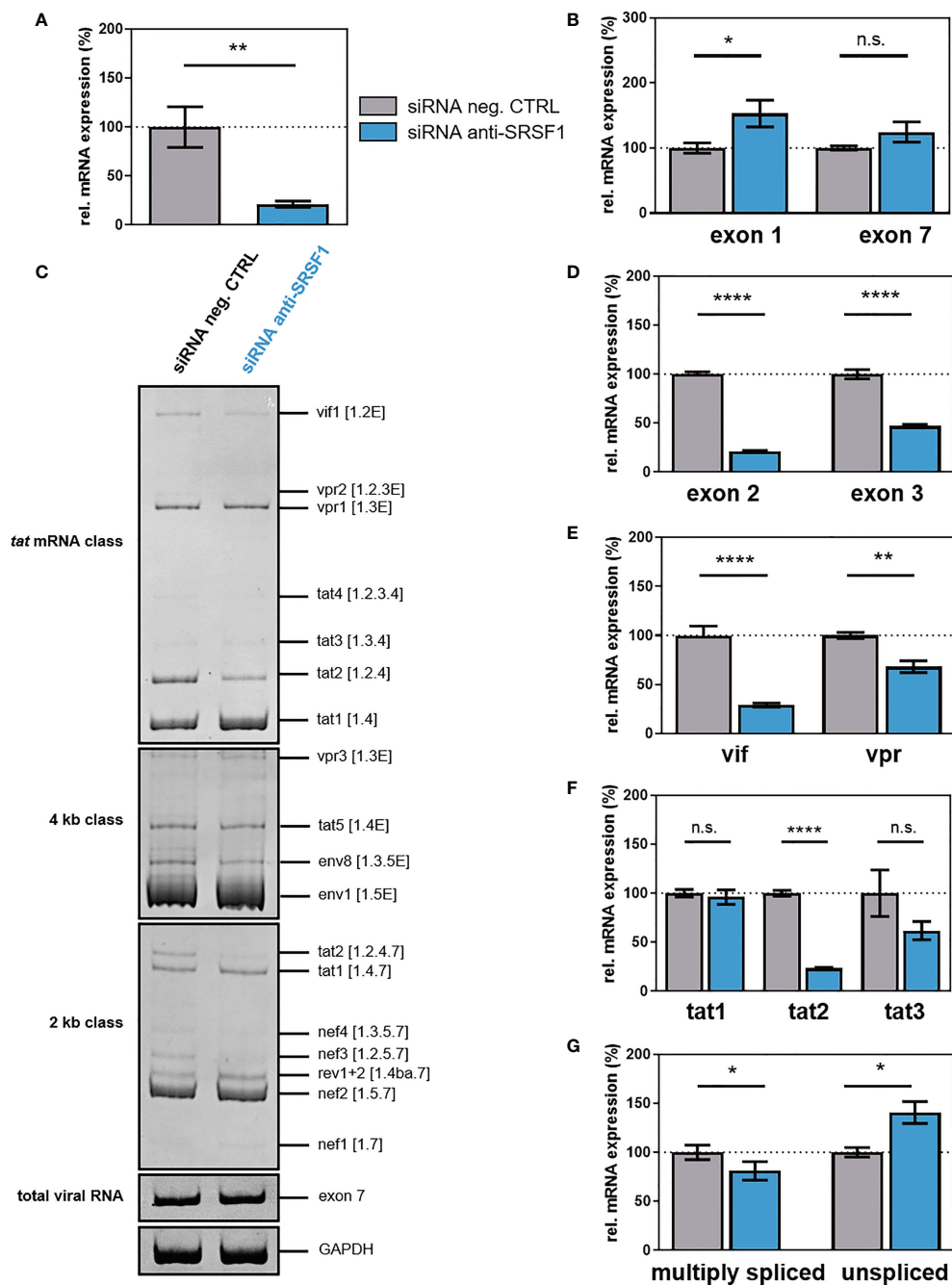


FIGURE 7

siRNA-mediated knockdown of SRSF1 affects HIV-1 LTR transcription and splice site usage. HEK293T cells were transfected with the proviral clone pNL4-3 PI952 and anti-SRSF1 siRNA or an siRNA negative control. Seventy-two hours post-transfection, cells were harvested and RNA and viral supernatant was isolated. Isolated RNA was subjected to RT-qPCR. **(A, B)** Relative mRNA expression levels of **(A)** *SRSF1* and **(B)** exon 1- and exon 7-containing mRNAs (total viral mRNA) normalized to GAPDH expression. **(C)** Analysis of viral splicing pattern upon SRSF1 knockdown. Isolated RNA was subjected to RT-PCR analysis using the indicated primer pairs for the 2-kb, 4-kb, and *tat* mRNA class (Supplementary Table 1, Supplementary Table 2, and Supplementary Figure 4). HIV-1 transcript isoforms are depicted on the right according to Purcell and Martin (36). To compare total RNA amounts, separate RT-PCRs amplifying HIV-1 exon 7-containing transcripts as well as cellular GAPDH were performed. PCR amplicons were separated on a 12% non-denaturing polyacrylamide gel. **(D–G)** Relative expression levels of **(D)** exon 2- and exon 3-containing, **(E)** *vif* and *vpr*, **(F)** *tat1*, *tat2*, and *tat3*, and **(G)** multiply spliced and unspliced mRNAs. HIV-1 mRNAs were analyzed using the indicated primers (Supplementary Table 1, Supplementary Table 2, and Supplementary Figure 4). The mRNA expression of NL4-3 PI952 was set to 100%, and the relative splice site usage was normalized to total viral mRNA levels (exon 7-containing mRNAs). Unpaired two-tailed t-tests were calculated to determine whether the difference between the group of samples reached the level of statistical significance (\* $p < 0.05$ , \*\* $p < 0.01$ , \*\*\*\* $p < 0.0001$  and ns, not significant). Mean ( $\pm$  SEM) of  $n = 4$  biological replicates is depicted for **(A)**, **(B)**, and **(D–G)**. For **(C)**, a representative gel is shown.

To evaluate the impact of IFN-mediated repression of *SRSF1* on HIV-1 post-integration steps, we transiently silenced endogenous *SRSF1* expression using a siRNA-mediated knockdown approach. HEK293T cells were transiently co-transfected with a plasmid coding for the HIV-1 laboratory strain NL4-3 PI952 (pNL4-3 PI952) (111) and an *SRSF1*-specific siRNA or a siRNA negative control. Seventy-two hours post-transfection, cells and the virus-containing supernatant were harvested. Knockdown efficiency was verified *via* One-Step RT-qPCR, revealing a significant knockdown of *SRSF1* gene expression of 85% when compared to the negative control siRNA (Figure 7A). Intracellular total viral mRNA levels were determined by means of exon 1- or exon 7-containing mRNAs, which are present in all viral mRNA isoforms (36). Upon knockdown of *SRSF1*, exon 1-containing mRNA transcripts were significantly increased by 1.5-fold (Figure 7B). Thus, depleted levels of *SRSF1* could potentially result in less competition in TAR binding, thereby increasing LTR promoter activity.

Next, we investigated whether knockdown of *SRSF1* might affect HIV-1 alternative splicing and performed semi-quantitative RT-PCR focusing on viral intron-less (2 kb) and intron-containing (4 kb) mRNA classes as well as *tat*-specific mRNA isoforms. No changes in the viral splicing pattern were observed in the 4-kb mRNA class upon depleted levels of *SRSF1* (Figure 7C). In the 2-kb mRNA class, *tat2* and *nef3* mRNA expression was reduced, while in the *tat*-specific mRNA class, *vif1* and *tat2* levels were decreased (Figure 7C). The formation of *vif1*, *tat2*, and *nef3* mRNA, which all contain non-coding leader exon 2, requires splicing from splice donor (SD) 1 to splice acceptor (SA) 1 (36). Thus, an effect of depleted levels of *SRSF1* on the frequency of SA1 splice site recognition and usage was suggested. Alterations in the expression of specific HIV-1 mRNA transcripts were also quantitatively confirmed by RT-qPCR using transcript-specific primer pairs (Figures 7D–G, Supplementary Table 1, Supplementary Table 2, Supplementary Figure 4). The frequency of transcripts containing the non-coding leader exon 2 and 3 was significantly reduced by 5- and 2-fold, respectively (Figure 7D). Knockdown of *SRSF1* resulted in a 3.6-fold downregulation of *vif* mRNA expression (Figure 7E). Since it has previously been shown that reduced Vif protein levels result in viral replication failure (112–114), the substantial loss in *vif* mRNA could potentially severely affect viral replication. The formation of *vif* mRNA requires splicing from SA1 to SD1 (36). Thus, the observed repression in exon 2 inclusion and *vif* mRNA levels suggested a reduced splicing frequency at SA1. Since the SRE ESE M1/M2 was shown to regulate splice site usage at SA1 and is a known target of *SRSF1* (79), it was suggested that lower levels of *SRSF1* resulted in a lower recognition of SA1 and thus induced a decrease in *vif* and exon 2-containing mRNA transcripts. Furthermore, *vpr* mRNA expression was decreased by 1.4-fold (Figure 7E). Splicing from SD1 to SA2 is required for

the generation of *vpr* mRNA (36). The observed reduction in exon 3 inclusion and *vpr* mRNA expression suggested a reduced splice site usage at SA2. However, no *SRSF1*-bound SRE involved in the regulation of SA2 splice site usage has yet been identified. While mRNA levels of *tat1* were not altered upon *SRSF1* knockdown, both *tat2* and *tat3* mRNAs were repressed by four- and twofold, respectively; however, only the reduction of *tat2* was significant (Figure 7F). Splicing from SD4 to SA7 is required for the formation of *tat1*, *tat2*, and *tat3* mRNA. Furthermore, splicing from SD1 to SA3 (*tat1* mRNA), from SD1 to SA1 and SD2 to SA3 (*tat2* mRNA), and from SD1 to SA2 and SD3 to SA3 (*tat3* mRNA) is necessary for the generation of the respective mRNAs (36). Since the levels of multiply spliced mRNAs (spliced from SD4 to SA7) were significantly decreased by 1.3-fold, while the levels of unspliced viral mRNAs (containing intron 1) were significantly increased by 1.4-fold, knockdown of *SRSF1* was suggested to shift the ratio towards unspliced mRNAs (Figure 7G). The suggested decrease in splicing events at SA1 and SA2 were in accordance with the increased amount of unspliced mRNAs. The decrease in multiply spliced mRNAs indicates reduced SD4–SA7 splicing, suggesting a possible involvement of the *SRSF1*-bound SRE ESE3, which regulates splicing at SA7 (80).

To investigate whether *SRSF1* knockdown and the observed effects on HIV-1 LTR transcription and alternative splice site usage would affect viral infectivity, RPE-ISRE luc reporter cells were transiently co-transfected with a plasmid expressing the HIV-1 laboratory strain NL4-3 (pNL4-3) (115) and a *SRSF1*-specific siRNA or a siRNA negative control. Forty-eight hours post-transfection supernatants of transfected cells were collected. TZM-bl cells were then infected with virus-containing cellular supernatant. TZM-bl cells harbor reporter genes for firefly luciferase and  $\beta$ -galactosidase under the control of the HIV-1 LTR promoter (116). Since the LTR-dependent luciferase activity and  $\beta$ -galactosidase of the reporter cells was significantly increased by up to 1.7-fold, low *SRSF1* levels were facilitating viral infectivity (Figures 8A, B). Interestingly, the observed changes in HIV-1 splice site usage, including a 3.6-fold reduction in *vif* mRNA expression (Figure 7E), did not impede viral infectivity.

Only a marginal and nonsignificant 1.1-fold increase in p24-CA levels was detected upon *SRSF1* knockdown (Figure 8C). RT-qPCR analysis with viral RNA extracted from the cellular supernatant was performed, revealing a 1.4-fold increase in viral copies, albeit not significant (Figure 8D).

To demonstrate the effect of Vif reduction and increased LTR activity in the presence of the restriction factor APOBEC3G, HEK293T- and APOBEC3G-expressing derivative cells were co-transfected with HIV-1 encoding plasmid DNA and siRNA against *SRSF1* (Figure 8E). The virus-containing supernatants were used to infect TZM-bl reporter cells. Compared to parental cells, the presence of APOBEC3G significantly reduced the infectivity of the virus particles.

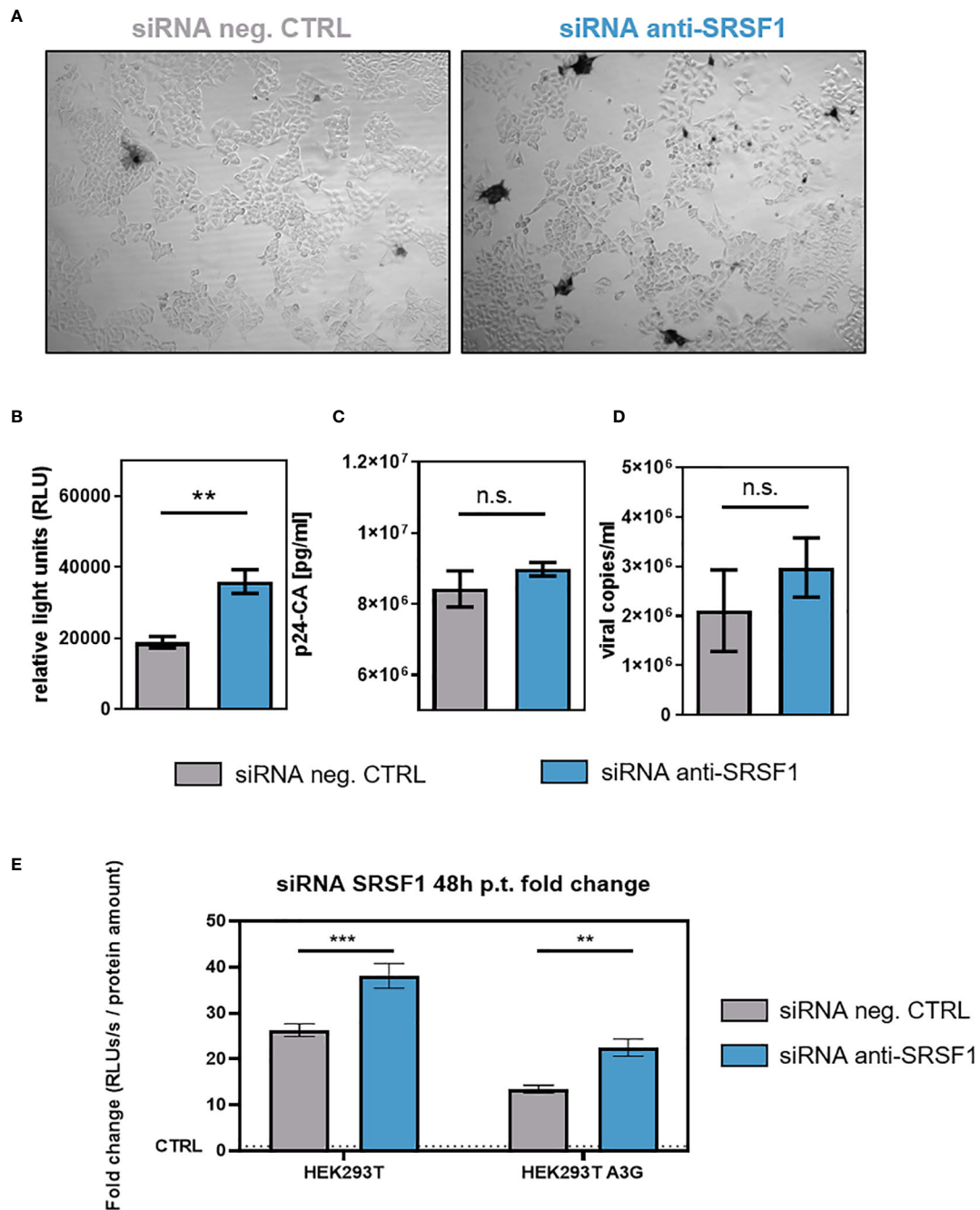


FIGURE 8

Impact of siRNA-based knockdown of SRSF1 on HIV-1 infectivity and virus production. RPE-ISRE luc cells were transfected with a plasmid coding for the proviral clone NL4-3 (AD8) (pNL4-3 AD8) and the indicated siRNA. Seventy-two hours post-transfection, cellular supernatant was harvested. (A, B) Viral infectivity was determined via TZM-bl assay. (A) Infected TZM-bl cells were stained with X-Gal. (B) Luciferase activity was determined measuring relative light units (RLUs). (C) p24-CA ELISA was performed to determine p24-CA levels in the cellular supernatant. (D) Cellular supernatant was used to determine viral copy number per milliliter. RT-qPCR was performed analyzing absolute expression levels of exon 7-containing transcripts (total viral mRNA). Statistical significance was determined using unpaired two-tailed *t*-tests (\*\**p* < 0.01). Mean (± SEM) of *n* = 4 biological replicates is shown for (B), (C), and (D). (E) HEK293T- and HEK293T APOBEC3G-expressing cells were seeded in poly-L-lysine (Sigma-Aldrich) pre-coated wells. Cells were transiently transfected with the proviral clone pNL4-3 and 12.8 nM of the indicated siRNA. Supernatants were harvested 48 h post-transfection and applied to TZM-bl cells. Forty-eight hours post-infection, cells were lysed for luciferase assay. The RLUs/s were normalized to whole protein amounts as determined using Bradford assay. The fold change is normalized to the signal of uninfected TZM-bl cells. Mean (± SEM) of *n* = 4 biological replicates and *n* = 2 technical replicates is shown. The significance was analyzed using two-way ANOVA (\*\**p* < 0.01, \*\*\**p* < 0.001, and ns, not significant).



Interestingly, however, SRSF1 knockdown still led to a significant increase in infectivity (Figure 8E), which was in agreement with previous observations (Figure 8B).

In conclusion, although siRNA-mediated knockdown of SRSF1 predominantly lowered *vif* mRNA expression, low SRSF1 levels resulted in facilitated viral infectivity, most likely due to increased LTR promoter activity. Thus, suppression of SRSF1 levels, as observed in the early immune response to an HIV-1 infection, could potentially facilitate HIV-1 infectivity and the establishment of a systemic infection.

## Overexpression of SRSF1 levels negatively affects HIV-1 replication

IFN $\alpha$ 14 stimulation of THP-1 cells and primary macrophages resulted in SRSF1 repression (Figures 4–6) and higher infectivity (Figures 7 and 8). To assess whether elevated levels of SRSF1 would negatively affect HIV-1 post-integration steps, we transiently transfected HEK293T cells with a plasmid expressing an HIV-1 laboratory strain (pNL4-3 PI952) (111) and an expression plasmid coding for FLAG-tagged SRSF1 (pcDNA-FLAG-SF2) (117) or an empty vector [pcDNA3.1(+)] as mock control. After 72 h, cellular RNA and virus-containing supernatant were harvested. One-Step RT-qPCR analysis revealed enhanced levels of *SRSF1* by multiple orders of magnitude (Figure 9A). Furthermore, protein expression and nuclear localization were confirmed using immune fluorescence microscopy (Supplementary Figure 5). As determined by RT-qPCR using primer pairs amplifying exon 1- or exon 7-containing mRNAs (Supplementary Figure 4), overexpression of SRSF1 induced a significant 1.7-fold reduction in total viral mRNA levels (determined by both exon 1- and exon 7-containing mRNAs) (Figure 9B). Increased levels of SRSF1 were thus suggested to inhibit LTR transcription, which was in accordance with previous data (78, 82).

Examining the viral splicing patterns *via* semi-quantitative RT-PCR, significant changes in all HIV-1 mRNA classes were observed upon overexpression of SRSF1 (Figure 9E). Increased levels of *vif*1, *vpr*1-2, and *tat*2-4 (tat mRNA class); *tat*2, *nef*1, and *nef*5 (2-kb class); and *vpr*3, *tat*5, and *tat*8 (4-kb class) were detected, while the transcript levels of *tat*1 (tat mRNA class), *tat*1 and *nef*2 (2-kb class), and *env*1 (4-kb class) were reduced (Figure 9C). Alterations in the expression of specific HIV-1 mRNA transcripts were also quantitatively confirmed by RT-qPCR using transcript-specific primer pairs (Figures 9D–G; Supplementary Tables 1, 2, Supplementary Figure 4). While the inclusion of non-coding leader exon 2 was not altered upon elevated levels of SRSF1, the inclusion of non-coding leader exon 3 was significantly decreased by threefold (Figure 9D). The mRNA expression levels of *vif* (spliced from SD1 to SA1) and *vpr* (spliced from SD1 to SA2), which crucially depend on the recognition of SA1 and SA2, were strongly increased by 12- and

16-fold, respectively (Figure 9E). These findings suggested that the splicing frequency at SA1 and SA2 was substantially increased, whereas splicing at SD2 and SD3 was inhibited. Since cross-exon interactions play a crucial role in exon 2 and exon 3 definition, it is likely that elevated levels of SRSF1 affect cross-exon interactions between SA1 and SD2, and SA3 and SD3. Furthermore, overexpression of SRSF1 induced a threefold decrease in *tat*1 mRNA levels, while the levels of *tat*2 and *tat*3 mRNA, which are also dependent on SA1 and SA2 recognition, increased by 2.3- and 4-fold, respectively (Figure 9F). The increased splice site usage at SA1 and SA2 was in accordance with the observed 1.6-fold decrease in unspliced mRNA transcripts (Figure 9G). An effect of elevated SRSF1 levels on the splicing frequency at SA7 was unlikely since the levels of multiply spliced mRNAs (spliced from SD4 to SA7) were not significantly altered (Figure 9G).

To analyze whether overexpression of SRSF1 and the concomitant changes in HIV-1 LTR transcription and alternative splice site usage would affect viral infectivity, TZM-bl reporter cells were infected with the virus-containing cellular supernatant. High levels of SRSF1 resulted in a strong decrease in infectious viral titers by X-Gal staining of infected TZM-bl cells (Figure 10A). As confirmed with a quantitative luciferase assay, a 4.1-fold significantly lower infectivity was observed (Figure 10B).

The levels of p24-CA were significantly lower (1.2-fold) upon SRSF1 overexpression (Figure 10C). The number of viral copies in the supernatant was determined *via* RT-qPCR analysis, revealing 1.4-fold lower (but not significant) levels when compared to the mock control (Figure 10D).

In conclusion, plasmid-driven overexpression of SRSF1 substantially altered the balanced ratios of HIV-1 mRNA transcripts and negatively affected Tat-LTR transcription. Contrary to reduced SRSF1 levels, overexpression significantly impaired HIV-1 particle production and infectivity.

## Discussion

Type I IFNs (IFN-I) play a key role in the early immune defense against viral infections (1, 2). Their mode of action includes immunomodulatory functions and the upregulation of hundreds of IFN-stimulated genes (ISGs), thereby establishing an antiviral state in infected host and bystander cells. Furthermore, they induce the downregulation of host factors essential for viral replication, which are termed IRepGs (29, 30). In this study, we were able to identify the cellular splicing factor *SRSF1* as an IFN-I-regulated gene, crucially affecting HIV-1 post-integration steps at the level of LTR transcription, alternative splicing, and virus production.

Based on the increased ISG expression in PBMCs (Figure 2A) and LPMCs (87) of acutely and chronically HIV-1-infected individuals, we confirmed both of our patient cohorts

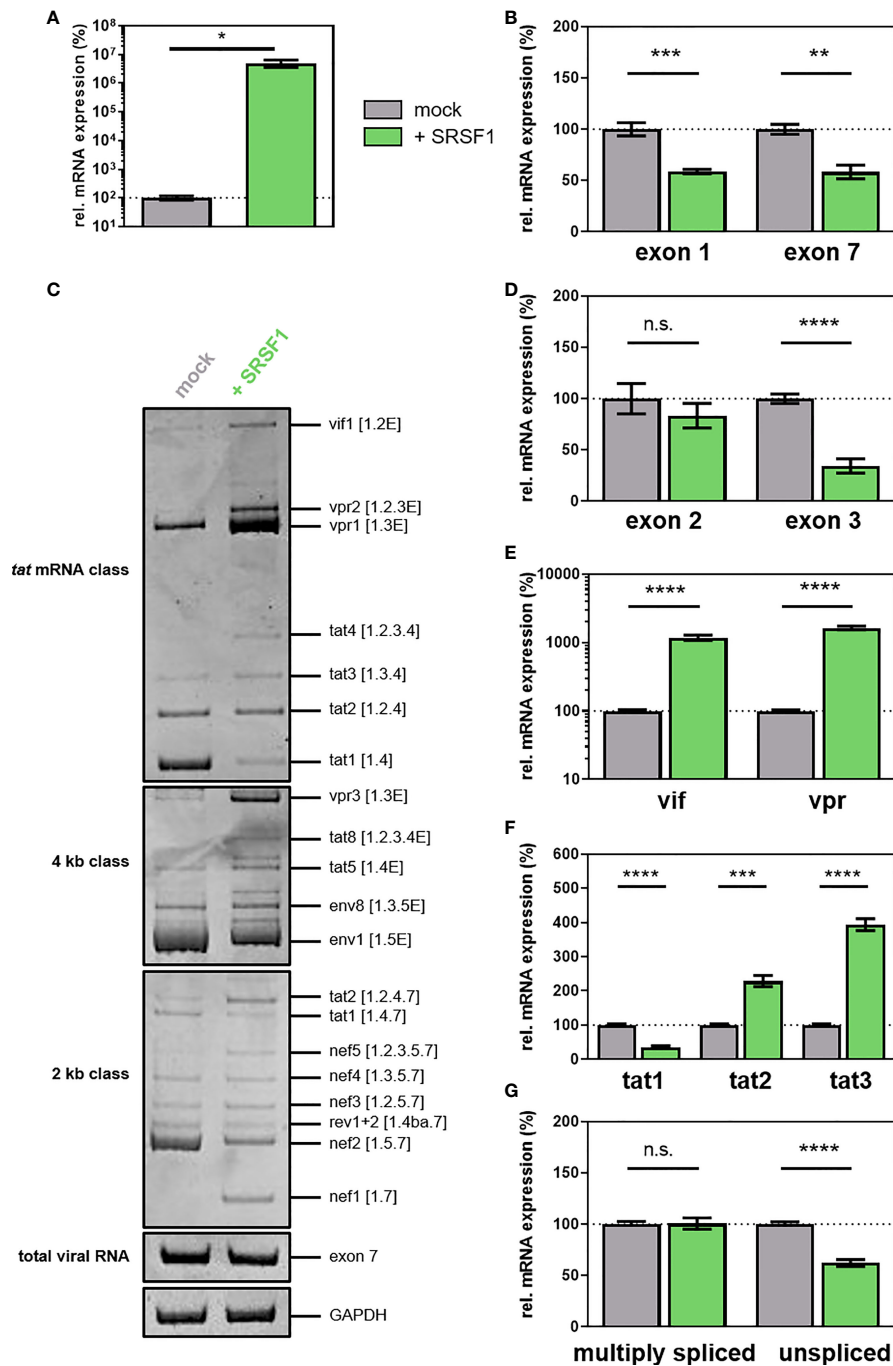


FIGURE 9

(A–G) Overexpression of SRSF1 affects HIV-1 LTR transcription and alternative splice site usage. HEK293T cells were transiently transfected with a plasmid coding for the proviral clone NL4-3 PI952 (pNL4-3 PI952) and a plasmid expressing FLAG-tagged SRSF1 (pcDNA-FLAG-SF2) or an empty vector [pcDNA3.1(+)] as mock control. Cellular RNA and cell culture supernatant were harvested 72 h post-transfection and subjected to further analysis. (A, B) RT-qPCR was performed to determine relative mRNA expression levels of (A) *SRSF1* and (B) exon 1- and exon 7-containing mRNAs (total viral mRNA). GAPDH was used for normalization. (C) RT-PCR was performed using the indicated primer pairs covering the viral mRNA isoforms of the 2-kb, 4-kb, and *tat* mRNA class (Supplementary Tables 1, 2 and Supplementary Figure 4). HIV-1 transcript isoforms are indicated according to Purcell and Martin (36). HIV-1 exon 7-containing transcripts as well as cellular GAPDH were included as loading controls. PCR amplicons were separated on a 12% non-denaturing polyacrylamide gel. (D, G) Total RNA was subjected to RT-qPCR to measure relative mRNA expression levels of (D) exon 2- and exon 3-containing, (E) *vif* and *vpr*, (F) *tat1*, *tat2*, and *tat3*, and (G) multiply spliced and unspliced mRNAs using the indicated primers. Relative viral splice site usage was normalized to exon 7-containing mRNAs (total viral RNA). Unpaired two-tailed *t*-tests were used to calculate statistical significance (\* $p < 0.05$ , \*\* $p < 0.01$ , \*\*\* $p < 0.001$ , \*\*\*\* $p < 0.0001$ ). Mean ( $\pm$  SEM) of  $n = 4$  biological replicates is depicted for (A, B) and (D–G). For (C), a representative gel is shown. ns is not significant.

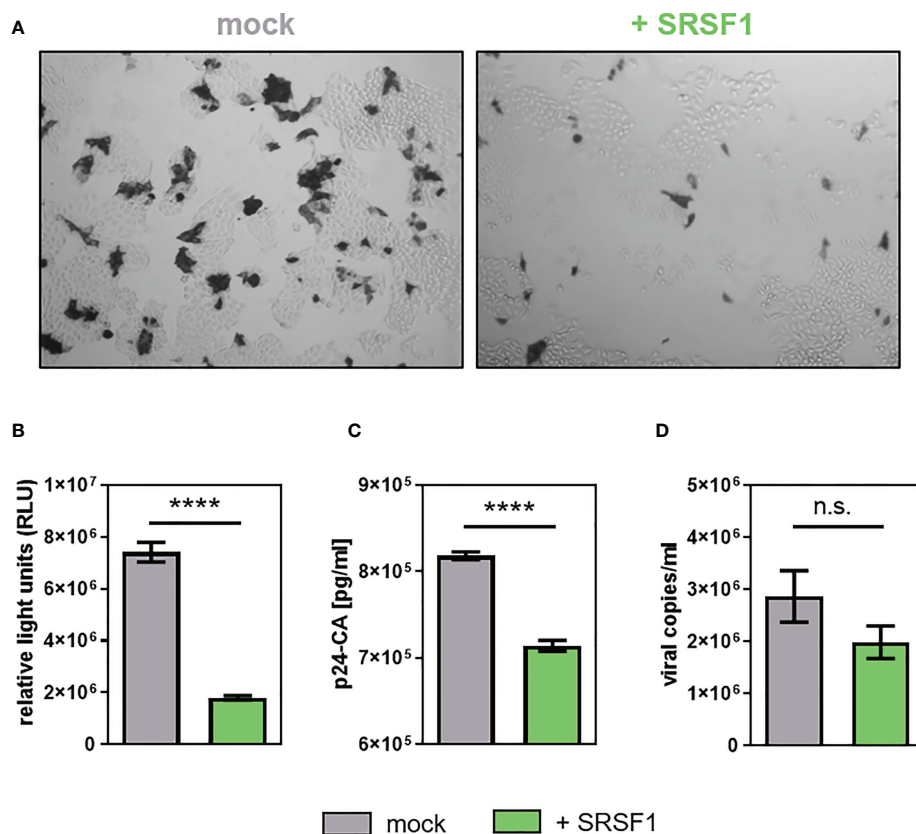


FIGURE 10

Overexpression of SRSF1 affects HIV-1 infectivity and viral particle production. HEK293T cells were co-transfected with a plasmid coding for the proviral clone NL4-3 PI952 (pNL4-3 PI952) (371) and a plasmid coding for FLAG-tagged SRSF1 (pcDNA-FLAG-SF2) or an empty vector [pcDNA3.1(+)] as mock control. (A, B) Seventy-two hours post-transfection, the cell culture supernatant was used to determine viral infectious titers using T2M-bl reporter cells. (A) X-Gal staining of T2M-bl cells incubated with the cellular supernatant. (B) Measurement of luciferase activity. (C) Viral RNA extracted from the supernatant was subjected to RT-qPCR to quantify absolute expression levels of exon 7-containing transcripts (total viral mRNA). (D) p24-CA ELISA was performed to determine viral particle production. Statistical significance was calculated using unpaired two-tailed *t*-tests (\*\*\*\* $p < 0.0001$  and ns, not significant). Mean ( $\pm$  SEM) of  $n = 4$  biological replicates is depicted for (B–D).

as being representative. Interestingly, we found the *ISG15* mRNA expression to be lower in ART-treated patients when compared to HIV-1-infected treatment-naïve individuals in PBMCs (Figure 2A). Indeed, it has been shown previously that in LPMCs of patients under ART treatment, ISG levels were comparable to healthy donors (87). It was shown that more than 4,000 genes are differentially expressed (118) and the IFN-induced JAK-STAT signaling pathway and several ISGs, such as *ISG15*, *Mx2*, or *IFITM1*, were downregulated following ART treatment. However, whether the low ISG level in our ART-treated cohort might result from a decrease in inflammation or from the administered drug needs further investigation.

During our initial screen, we investigated differences in the expression levels of *SRSF* transcripts in LPMCs of healthy donors and HIV-1-infected individuals, either treatment-naïve or under ART treatment. Specific *SRSF* transcript levels,

particularly *SRSF1*, were significantly lower upon HIV-1 infection (Figure 1A). These findings implied a direct or indirect effect of the HIV-1 infection on the gene expression of specific *SRSF* transcripts, potentially as a consequence of the IFN signaling. Supporting this hypothesis, a significant correlation was observed between the induction of *ISG15* mRNA expression and the repression of *SRSF1* mRNA levels in PBMCs of acutely HIV-1-infected patients (Figure 2F). Thus, the strong upregulation of IFN-I and subsequent induction of ISGs during the early inflammation in response to an HIV-1 infection (23) could potentially directly or indirectly result in the repression of *SRSF1*, suggesting a potential role of *SRSF1* as IRepG.

Interestingly, no significant differences were observed in the expression levels of most *SRSFs* when comparing LPMCs of ART-treated patients and healthy donors (Figure 1B). The

expression levels of *SRSF1* mRNA, which were reduced by 2-fold upon HIV-1 infection (Figure 1A), were even elevated by 1.2-fold upon ART treatment when compared to uninfected donors. Remarkably, while *SRSF1* transcript levels were restored upon ART treatment in gut LPMCs, this effect was not observed in PBMCs, indicating a tissue-dependent specificity (Figure 2C). This discrepancy could possibly be explained through the phenotypical and functional differences between the two immune cell populations. PBMCs and LPMCs reside within a strongly differing micro-environment, include a different composition of immune cells, and express distinct cytokines and receptors (119–127).

A significant time-dependent repression in *SRSF1* mRNA levels was observed upon stimulation with IFN-I in THP-1 macrophages, Jurkat T cells, and MDMs (Figures 4, 5). Since the effect on *SRSF1* mRNA expression varied greatly between cell types, and between transformed cell lines and primary cells, the IFN-I-mediated repression seemed to underlie cell-type-specific characteristics, such as the expression pattern of co-regulatory factors. The physiological relevance of primary human cells is certainly higher than transformed cell lines, since they provide a closer resemblance to physiological conditions (128, 129). Since treatment with IFN $\gamma$  only led to a negligible effect on *SRSF1* mRNA expression in THP-1 macrophages when compared to IFN $\alpha$ 2 or IFN $\alpha$ 14, a preferentially IFN-I-specific effect was implied (Figures 4, 5). However, while binding two distinct receptors and signaling *via* different pathways (2, 8), cross-talk between IFN-I and IFN-II has been observed (130–132).

The observed lower levels of *SRSF1* mRNA transcripts upon HIV-1 infection in LPMCs and PBMCs, as well as the time-dependent downregulation in *SRSF1* mRNA in various cell types upon stimulation with IFN-I, suggested *SRSF1* to represent an IRepG. However, prior to the strong downregulation upon stimulation with IFN $\alpha$ 2 and IFN $\alpha$ 14 in THP-1 macrophages, an increase in *SRSF1* mRNA expression was detected (Figures 4A, B, right panel). The method of 4sU tagging, which allows the analysis of RNA synthesis and degradation, as well as transcription factor functions (30, 108–110), confirmed a strong increase in *SRSF1* mRNA expression prior to the downregulation and revealed the changes in gene expression to most likely occur on the transcriptional level (Figure 6). Other regulatory mechanisms, however, might potentially be involved in the biphasic expression pattern. *SRSF1* was shown to be a direct transcriptional target of the oncogenic transcription factor *Myc* (133, 134). Since *Myc* expression was shown to be reduced by elevated levels of IFN-I (135–137), the observed reduction in *SRSF1* mRNA expression could potentially result from depleted *Myc* levels. Furthermore, *SRSF1* was shown to maintain homeostasis through an autoregulatory feedback loop (138, 139). Since deregulation of *SRSF1* was shown to be involved in tumorigenesis (133) (140, 141), tight regulation of *SRSF1* expression is important for

normal cell physiology. The most abundant *SRSF1* transcript isoform is the productively translated and intron-containing isoform 1 (139). Upon elevated levels of *SRSF1*, the degradation of *SRSF1* transcripts *via* RNA surveillance pathways, such as nonsense-mediated decay (NMD), is induced through the removal of introns (77, 138, 142). Thus, upon strongly elevated levels of freshly synthesized *SRSF1* mRNA, the negative feedback loop could induce a higher frequency in intron removal, possibly resulting in the observed strong downregulation in *SRSF1* mRNA transcripts at later time points. Furthermore, *SRSF1* activity and subcellular localization is regulated *via* phosphorylation (77, 143). Only partially phosphorylated *SRSF1* binds its RNA target sequences with high affinity, while unphosphorylated or fully phosphorylated *SRSF1* only has low binding affinities (60). Thus, an interaction between IFN-I-signaling and proteins regulating *SRSF1* phosphorylation or dephosphorylation, affecting *SRSF1* activity and localization, cannot be excluded.

*SRSF1* consists of two RRM, providing the RNA-binding specificity, and a relatively short RS domain (54). The purine-rich pentamer GGAGA was identified as *SRSF1* consensus motif *via in vivo* mapping (76, 77). Interestingly, while *SRSF1* mainly binds in ESE regions, introns contain a high number of potential binding sites (54). *SRSF1* was previously shown to regulate multiple steps of HIV-1 RNA processing, including alternative splice site usage (78–80) and LTR promoter activity (83, 84), thus hinting at an important function of *SRSF1* in HIV-1 RNA processing and replication. *SRSF1* and the viral protein Tat competitively bind to a binding sequence within the hairpin structure of the TAR region on the LTR promoter (83). While increased levels of *SRSF1* were shown to significantly impede Tat-activated LTR transcription, depleted levels resulted in enhanced LTR promoter activity (83, 84). In agreement with these data, we could show that siRNA-mediated knockdown of *SRSF1* resulted in increased total viral mRNA transcript levels and thus HIV-1 LTR transcriptional activity (Figure 8), while *SRSF1* overexpression led to a significant reduction in HIV-1 mRNA expression (Figure 10). Hence, a direct effect on *SRSF1* on HIV-1 LTR transcription was suggested. Furthermore, alternative splice site usage was crucially affected by altered *SRSF1* levels. Several SREs on the viral pre-mRNA were shown to be targeted by *SRSF1*, which are ESE M1/M2 (79), GAR ESE (78), and ESE3 (80), thereby enhancing the recognition of the proximal splice sites. Both overexpression and knockdown of *SRSF1* led to significant alterations in the ratio of multiply spliced (spliced from SD4 to SA7) to unspliced (intron 1 containing) mRNAs (Figures 7G and 9G). Overexpression of *SRSF1* resulted in decreased levels of unspliced mRNAs but unaltered transcript levels of multiply spliced mRNAs, while knockdown shifted the ratio towards unspliced mRNAs. These findings were in agreement with *SRSF1* enhancing splice site usage when binding SREs from an exonic position (61–63). Binding of *SRSF1* to ESE3, which is located downstream of SA7 (80, 81), promotes the recruitment of U2AF65 to the SA, thus increasing



splicing frequency at SA7 (81). The observed decrease in multiply spliced mRNAs upon SRSF1 knockdown might thus be explained through fewer splicing events at SA7 due to reduced SRSF1-mediated stabilization of U2 snRNP binding to the SA. Unaltered levels of multiply spliced mRNAs upon overexpression of SRSF1 were in accordance with a previous observation, showing that high levels of SRSF1 did not result in increased splicing frequency at SA7, possibly due to low binding affinity (81).

Cross-exon interactions play a key role in the recognition of exon 2 and exon 3 and concomitantly in the formation of *vif* and *vpr* mRNA (95, 144). Binding of the U1 snRNP to the 5'-SD, which stabilizes the binding of U2 snRNP to the branch point sequence and initiates the formation of an exon recognition complex (145), activates the upstream 3'-SA. We found that knockdown of SRSF1 induced a strong decrease in exon 2 inclusion and *vif* mRNA expression (Figures 7D, E), thus suggesting a strong reduction in splicing frequency at SA1. Since SRSF1 overexpression resulted in strongly increased *vif* mRNA levels, but not exon 2 inclusion (Figures 9D, E), splicing frequency at SA1 was likely enhanced, while splicing at SD2 and most likely at the alternative splice site SD2b (114) was blocked. ESE M1/M2 is located upstream of SD2 and was shown to promote the recognition of exon 2 via enhanced cross-exon interactions upon binding of SRSF1 (79). Thus, increased levels of SRSF1 likely resulted in increased recognition of SD2, thereby enhancing cross-exon interactions between SD2 and SA1. Depleted levels of SRSF1 resulted in fewer binding to ESE M1/M2, thereby resulting in lower splicing frequency at SA1, which, in turn, leads to reduced levels of exon 2 including and *vif* mRNA transcripts. Furthermore, while knockdown of SRSF1 resulted in strongly reduced exon 3-containing and *vpr* mRNAs (Figures 7D, E), overexpression concomitantly induced *vpr* mRNA expression but reduced exon 3 inclusion (Figures 9D, E). Recognition of SD3 was likely increased upon elevated levels of SRSF1, resulting in enhanced cross-exon interactions and thus splicing frequency at SA2. Impaired binding of U1 snRNP to SD3 could presumably lead to reduced exon 3 spanning cross-exon interactions. However, no SREs targeted by SRSF1 have been identified so far in proximity of SD3. The suggested reduction in splicing frequency at SA1 and SA2 upon SRSF1 knockdown was further sustained by the reduction of other exon 2 (*tat2* and *nef3*)- and exon 3 (*tat3* and *env8*)-containing mRNA levels. Moreover, induced mRNA levels of exon 2- and exon 3-containing mRNAs (*vpr2*, *tat4*, *tat8*, and *nef5*) upon elevated levels of SRSF1 supported the assumed increase in splicing events at SA1 and SA2.

Increased levels of SRSF1 also induced the repression of *env1* and *nef2*, which are spliced from SD1 to SA4 (36). A direct involvement of the bidirectional GAR ESE, which is located downstream of SA5 and was shown to regulate splicing frequency at SA4 (78, 146), was suggested. Upon binding of SRSF1 to GAR ESE, the recruitment of U1 snRNP to SD4 is enhanced, which increases splicing events at the upstream SA4 and SA5 (78, 146). However, in this study, reduced splicing

frequency at SA3 was observed upon elevated levels of SRSF1 (Figure 9F). This could possibly be explained through the high complexity and dynamic of the splicing process, which involves a large number of proteins and cellular splicing factors. Potential interactions with other factors might thus impede the stabilizing effect of SRSF1 on the binding of U1 snRNP to SD4.

Unbalanced splicing of HIV-1 mRNAs drastically impairs viral replication and infectivity. In particular, optimal Vif levels are essential for efficient viral replication in APOBEC3G-expressing cells (13, 112, 147). While low levels of Vif resulted in a complete failure in viral replication due to the inability to evade APOBEC3G-mediated effects (95), elevated levels of Vif strongly decreased viral infectivity through the inhibition of Gag processing at the nucleocapsid (112).

Although SRSF1 knockdown induced a strong reduction in *vif* mRNA expression, facilitated viral infectivity was observed (Figure 8). Most likely, the strong increase in all viral RNAs as determined by levels of exons 1 and 7 compensate for the reduced *vif* mRNA expression and prevails as the dominant phenotype. Drastically reduced viral infectivity was observed upon SRSF1 overexpression (Figure 10). In agreement with previous findings (112), strongly elevated levels of *vif* mRNA resulted in a significant decrease in viral infectivity due to modulation of the proteolytic Gag processing. A Vif-independent mechanism including a direct effect of SRSF1 or the interaction of other cellular factors, however, cannot be ruled out.

Virus production was marginally elevated upon depleted levels of SRSF1 (Figures 8C, D), which was in accordance with the increase in HIV-1 LTR promoter activity (Figure 7B) and Gag expression (148). Overexpression of SRSF1 led to strongly reduced viral copies in the cellular supernatant (Figure 10D), in accordance with the strong inhibition of LTR promoter activity (Figure 9B). In addition, further overexpression effects were described including reduced Tat, Gag, and Env levels as well as the aforementioned inhibition of Tat transactivation (148).

Knockdown of SRSF1 resulted in marginally increased HIV-1 LTR transcription and viral infectivity. Thus, the observed IFN-induced repression of SRSF1 does not seem to have an antiviral effect and might even be detrimental in the defense against HIV-1. In contrast, high SRSF1 levels drastically impaired HIV-1 LTR transcription and viral infectivity. Hence, elevated levels of SRSF1, which were observed at an early time point after IFN stimulation, might be part of the IFN-induced antiviral response in the early immune response to HIV-1.

Interestingly, a concomitant HIV-1 infection and IFN stimulation led to rapidly restored SRSF1 levels comparable to PBS-treated cells (Figure 4E). However, whether the virus-mediated alteration in *SRSF1* mRNA levels was due to sensing or a direct effect mediated by viral proteins remained unclear. At the chosen time point of IFN stimulation 16 h post-infection, viral integration is complete and viral mRNA expression is proceeding (96). To evaluate whether viral proteins might be involved in SRSF1 regulation, we performed a transient



transfection analysis. Overexpression of Vpr resulted in increased *ISG15* mRNA expression (Supplementary Figure 3A), which was in agreement with previous studies showing that Vpr is involved in the majority of changes in gene expression after HIV-1 infection (149). An NL4-3 derivative lacking Vpr only induced a limited *ISG15* response when compared to parental NL4-3 (Supplementary Figure 3). These findings strengthen the hypothesis of a direct interplay between HIV-1 accessory proteins and host cell proteins, resulting in enhanced SRSF1 expression levels after 24 and 48 h (Figure 4E). Furthermore, Tat and Rev (150, 151), as well as the accessory protein Nef, are among the early expressed HIV-1 proteins (152). Rev was previously shown to interact with SRSF1 via the splicing factor-associated protein p32 (153), which was suggested to ensure optimal stoichiometry of HIV-1 mRNA isoforms (154). Certain accessory proteins like Nef might, in addition to counteracting restriction factors such as tetherin (14, 155), also modulate signal transduction, autoregulation mechanisms, antigen presentation, or the expression of cell surface receptors [reviewed in (156–158)]. Since an autoregulatory feedback loop was shown to maintain homeostatic levels of SRSF1 (77, 138, 142), interaction of accessory proteins with this autoregulation might potentially explain the observed recovery in the mRNA expression kinetic (Figure 4E). Experimentally, it is challenging to distinguish between HIV-1-infected cells producing IFN $\alpha$  and bystander cells, which induce gene expression of HIV restriction factors prior to the infection, thus inhibiting pre-integration steps. Further experiments will be required to distinguish the effect of modulated SRSF1 levels between these two cell populations.

Aside from being a crucial regulator of several HIV-1 post-integration steps, SRSF1 has a much broader scope of action. Among a crucial role in cellular alternative splicing (143), SRSF1 regulates genome stability (159), translation (160), nuclear export (69), or the nonsense-mediated mRNA decay (NMD) pathway (161, 162). Loss of SRSF1 protein function resulted in G2 cell cycle arrest and induced apoptosis (163). Moreover, SRSF1 was defined as a proto-oncogene, since upregulation of SRSF1 favors the formation of a variety of cancers (133, 140, 141). Thus, the IFN-induced downregulation of *SRSF1* described in this manuscript might not only affect HIV-1 post-integration steps, but also a variety of other cellular functions. Restoring balanced levels of SRSF1 after IFN treatment is essential for normal cell physiology, as prolonged unbalanced levels might have detrimental consequences.

As key factor for efficient HIV-1 replication, alternative splicing has been investigated as a potential target for ART (148, 164). An interesting question that remains is whether drug targeting of SRSF1 could potentially result in viral inhibition. The drug IDC16 was shown to block the replication of CXCR4- and CCR5-tropic viruses, as well as clinical isolates via direct interaction with SRSF1 (165, 166). The indole derivative can significantly impair the ESE activity

of SRSF1 through binding of the RS domain and subsequently preventing its phosphorylation (165–167). Potential side effects of the drug are currently reviewed in *in vivo* studies. Current antiviral therapy is based on the inhibition of viral proteins, such as protease, integrase, or reverse transcriptase (168, 169). However, long-term use as well as inconsistent intake of these drugs can result in the emergence of drug-resistant mutations and can cause severe side effects (169). Thus, targeting cellular factors crucially involved in the regulation of HIV-1 post-integration steps may offer new approaches for antiviral therapy. However, the use of such drugs should be approached cautiously, due to the large number of cellular processes that are regulated by these factors.

This study had several limitations. We only had limited access to samples, in particular to those obtained from acutely infected individuals from different Fiebig stages (I–V). Factors such as age and gender, but also comorbidity and medication, nutrition, as well as other unknown environmental influences might have an impact on human gene expression including *ISG15* and *SRSF1* (142, 170–172). However, these data were not collected during this study and therefore cannot be used for further subgroup analysis. Another limitation of this study is the fact that SRSF1 knockdown and overexpression were performed in HEK293T cells. Although these cells are well established in the field, they do not represent natural HIV target cells. An efficient SRSF1 knockdown proved to be difficult in the course of the study, since, on the one hand, a complete knockout is lethal, while a minor knockdown is counteracted by an autoregulatory mechanism. Due to the technical complexity of achieving efficient SRSF1 knockdown, the question of its downregulation in natural host cells cannot be answered in this study and requires further research.

The different IFN $\alpha$  subtypes have been shown to exert different biological activities (173). Consistent with the observation that the IFN $\alpha$  subtypes induce different sets of ISGs (26), the different subtypes also showed clear differences in the ability to downregulate *SRSF1* mRNA expression (Figure 3B). While several IFN $\alpha$  subtypes elicit an antiviral activity suppressing HIV-1 infection, IFN $\alpha$ 14 was shown to be the most potent subtype against HIV-1 *ex vivo* and *in vivo* (26, 27). In contrast to IFN $\alpha$ 14, the subtype IFN $\alpha$ 2, which is the sole subtype in clinical use against HBV (28), elicited only weak anti-HIV-1 activity (26, 27). In an *in vivo* humanized mouse model, it was shown that combined treatment of ART and IFN $\alpha$ 14 led to a more efficient suppression in HIV-1 plasma viral load than ART treatment alone (174, 175). While a clinical study to test a concomitant administration of ART and IFN $\alpha$ 2 has been carried out (<https://clinicaltrials.gov/ct2/show/results/NCT02227277>), a benefit of subtype IFN $\alpha$ 14 when compared to IFN $\alpha$ 2 for a potential use in therapy might have a higher effectiveness. However, since IFN $\alpha$ 14 induces stronger intrinsic and innate immune responses (27), the administration of IFN $\alpha$ 14 could also potentially cause more severe side effects when compared to IFN $\alpha$ 2.

As a quintessence of this study, the IFN $\alpha$ -induced upregulation of HIV host restriction factors has been shown to severely limit viral replication (26, 27). In particular, pre-treatment with IFN $\alpha$  renders the cell into an antiviral state and inhibits numerous viral pre-integration steps (176). However, the IFN $\alpha$ -mediated deregulation of SRSF1 might at least partially direct the fate of viral replication and compensate for the antiviral activity by increasing the HIV-1 LTR transcription and virus production.

## Materials and methods

### Cell culture, transient transfection, and treatment

HEK293T, TZM-bl, Vero, and RPE ISRE-Luc reporter cells were maintained in Dulbecco's modified Eagle medium (Gibco) supplemented with 10% (v/v) heat-inactivated fetal calf serum (FCS) and 1% (v/v) penicillin–streptomycin (P/S, 10,000 U/ml, Gibco). Jurkat and THP-1 cells were maintained in Roswell Park Memorial Institute (RPMI) 1640 medium (Gibco) supplemented with 10% (Jurkat) or 20% (THP-1) (v/v) heat-inactivated fetal calf serum (FCS) and 1% (v/v) penicillin–streptomycin (10,000 U/ml, Gibco). THP-1 monocytes were treated with 100 nM 12-*O*-tetradecanoylphorbol-13-acetate (TPA) for 5 days to differentiate into macrophage-like cells. Differentiation was monitored *via* cell morphology and adhesion.

Transient transfection experiments were performed in six-well plates at  $2.5 \times 10^5$  HEK 293 T cells per well using TransIT<sup>®</sup>-LT1 transfection reagent (Mirus Bio LLC) according to the manufacturer's instructions unless indicated otherwise.

IFN $\alpha$  subtypes were produced as previously described (27); IFN $\gamma$  was purchased from PBL assay science (Piscataway). For the stimulation with IFN, 10 ng/ml of the respective IFN was added in fresh medium to the cells. The cells were then incubated at 37°C and 5% CO<sub>2</sub> for the indicated amount of time before being harvested. Ruxolitinib (*In vivogen*) was resuspended in DMSO and further diluted in aqueous buffer. THP-1 cells were treated with either 1  $\mu$ M Ruxolitinib or an equal volume of DMSO 1 h before infection. For each step involving media exchange, fresh Ruxolitinib was added.

The APOBEC3G-expressing HEK293T cells were previously stably transfected using the Sleeping Beauty system (177) and sorted in regard to their APOBEC3G expression.

### RNA isolation, quantitative, and semi-quantitative RT-PCR

The cells were harvested, and total RNA was isolated using the RNeasy Mini Kit (Qiagen) according to the manufacturer's

instructions. RNA concentration and quality were monitored *via* photometric measurement using NanoDrop2000c (Thermo Scientific). For reverse transcription (RT), 1  $\mu$ g of RNA was digested with 2 U of DNase I (NEB). After heat inactivation of the DNase at 70°C for 5 min, cDNA synthesis for infection experiments was performed for 60 min at 50°C and 15 min at 72°C using 200 U SuperScript III Reverse Transcriptase (Invitrogen), 40 U RNase Inhibitor Human Placenta (NEB), 50 pmol Oligo d(T)23 (NEB), and 10 pmol Deoxynucleotide Triphosphate Mix (Promega). For all other experiments, cDNA synthesis was performed for 60 min at 42°C and 5 min at 80°C using the ProtoScript II First Strand cDNA synthesis kit (NEB) according to the manufacturer's instructions. Quantitative RT-PCR analysis was performed using Luna<sup>®</sup> Universal qPCR Master Mix (NEB) and Rotor-Gene Q (Qiagen). Primers used for qPCR are listed in [Supplementary Table 2](#). ACTB or GAPDH was used as loading control for normalization. For qualitative analysis of HIV-1 mRNAs, PCR was performed using GoTaq G2 DNA Polymerase (Promega) according to the manufacturer's instructions. PCR products were separated on non-denaturing polyacrylamide gels (12%), stained with Midori green Advanced DNA stain (Nippon Genetics), and visualized with ADVANCED Fluorescence and ECL Imager (Intas Science Imaging).

Plasma HIV-1 RNA level was quantified using the RealTime HIV-1 m2000 test system (Abbott) according to manufacturer's instructions.

### IFN activity assay in the RPE ISRE-luc reporter cell line

A reporter cell line of human retinal pigment epithelial (RPE) cells, stably transfected with a plasmid containing the firefly luciferase reporter gene under the control of the IFN-stimulated response element (ISRE), was used to determine the activity of the different IFN $\alpha$  subtypes (27). Cells were seeded at  $1.5 \times 10^5$  cells per well in 12-well plates and incubated overnight. The next day, cells were stimulated with 10 ng/ml of the respective IFN $\alpha$  subtype for 5 h. Cells were then lysed with Passive lysis buffer (Promega) and frozen at -80°C overnight. After thawing, lysates were spun down and transferred to a white F96 Microwell plate (Nunc) before adding firefly luciferase substrate. Luminescent signal was measured using the GloMax<sup>®</sup> Multi Detection System (Promega).

### Preparation of virus stocks and infection

For the preparation of virus stocks,  $6.5 \times 10^6$  HEK293T cells were seeded in T175 flasks coated with 0.1% gelatin solution. The next day, cells were transiently transfected with 19  $\mu$ g of pNL4-3 or the respective proviral DNA using TransIT<sup>®</sup>-LT1 transfection reagent (Mirus Bio LLC) according to the

manufacturer's instructions. After 24 h, the cells were supplemented with Iscove's Modified Dulbecco's Medium [IMDM, 10% (v/v) FCS, and 1% (v/v) P/S] and incubated again overnight. The virus-containing supernatant was then purified by filtration through 0.30- $\mu$ m MACS SmartStrainers (Miltenyi Biotec), aliquoted, and stored at  $-80^{\circ}\text{C}$ . Differentiated THP-1 cells and Jurkat cells were infected with the R5-tropic NL4-3 (AD8) (1 MOI) or the dual tropic NL4-3 PI952 (1 MOI), respectively, with a spin inoculation for 2 h at  $1,500 \times g$ . Sixteen hours post-infection, indicated treatments were carried out.

## Protein isolation and Western blot

For protein isolation, cells were lysed with RIPA buffer [25 mM Tris-HCl (pH 7.6), 150 mM NaCl, 1% NP-40, 1% sodium deoxycholate, 0.1% SDS, and protease inhibitor cocktail (Roche)]. The lysates were subjected to SDS-PAGE under denaturing conditions in 12% polyacrylamide gels using the Bio-Rad Mini PROTEAN electrophoresis system (Bio-Rad). Gels were run for 90 min at 120 V in TGS running buffer [25 mM Tris, 192 mM glycine, and 0.1% SDS (v/v)]. NC membrane (pore size, 0.45 mm) was used for protein transfer using the Bio-Rad Mini PROTEAN blotting system (Bio-Rad). Proteins were transferred for 1 h at 300 mA in transfer buffer [25 mM Tris, 192 mM glycine, and 20% MeOH (v/v)]. The membrane was blocked in TBS-T [20 mM Tris-HCl, 150 mM NaCl, and 0.1% Tween-20 (v/v) (pH 7.5)] with 5% nonfat dry milk for 1 h at RT and then incubated overnight at  $4^{\circ}\text{C}$  with the primary antibody in TBS-T including 0.5% nonfat dry milk. The membrane was washed three times for 10 min in TBS-T. The horseradish peroxidase (HRP)-conjugated secondary antibody was added in TBS-T including 0.5% nonfat dry milk and incubated for 1 h at RT. The membrane was washed five times for 12 min with TBS-T before ECL chemiluminescent detection reagent (Amersham) was added and readout was performed with ADVANCED Fluorescence and ECL Imager (Intas Science Imaging). The following primary antibody was used: Mouse antibody specific for SRSF1 (32–4500) from Invitrogen. The following HRP-conjugated secondary antibody was used: anti-mouse HRP conjugate (315-035-048) from Jackson ImmunoResearch Laboratories Inc.

## p24-CA ELISA

For the quantification of HIV-1 p24-CA, a twin-site sandwich ELISA was performed as previously described (95). Briefly, Immuno 96 MicroWell plates (Nunc) were coated with  $\alpha$ -p24 polyclonal antibody (7.5  $\mu\text{g}/\text{ml}$  of D7320, Aalto Bio Reagents) in bicarbonate coating buffer ( $\text{NaHCO}_3$ , 100 mM,

pH 8.5) overnight at room temperature. The plates were washed with TBS and blocked with 2% non-fat dry milk powder in TBS for 1 h at room temperature. EMPIGEN twitterionic detergent (Sigma) was added to the samples for inactivation of HIV-1 and incubated for 30 min at  $56^{\circ}\text{C}$ . Capturing of p24 and subsequent washing were carried out according to the manufacturer's instructions (Aalto Bio Reagents). An alkaline phosphatase-conjugated  $\alpha$ -p24 monoclonal antibody (BC1071 AP, Aalto Bio Reagents) was used for quantification of p24. Readout was performed with the Spark<sup>®</sup> Microplate Reader (Tecan). Recombinant p24 was used to establish a p24 calibration curve.

## TZM-bl Luc assay and X-Gal staining

A total of 4,000 TZM-bl cells were seeded per well in 96-well plates and incubated overnight. One hundred microliters of the virus-containing supernatant was added to the cells, and the plates were incubated for 48 h. For the luciferase assay, 50  $\mu\text{l}$  of lysis juice (p.j.k.) was added after washing the plates with PBS, and the plates were shaken for 15 min at room temperature. Next, the plates were frozen for at least 1.5 h at  $-80^{\circ}\text{C}$  before being thawed. Lysates were resuspended and transferred to a white F96 Microwell plate (Nunc) for luminescent readout. One hundred microliters of beetle juice (p.j.k.) was added per well, and luminescence was measured with the Spark<sup>®</sup> Microplate Reader (Tecan) at an integration time of 2 s. For the X-Gal staining, cells were washed with PBS and fixed in 0.06% glutaraldehyde (Sigma) and 0.9% formaldehyde (Sigma) for 10 min at  $4^{\circ}\text{C}$ . Cells were washed twice with PBS and staining solution was added containing 400 mM  $\text{K}_3[\text{Fe}(\text{CN})_6]$ , 400 mM  $\text{K}_4[\text{Fe}(\text{CN})_6]$ , 100 mM  $\text{MgCl}_2$ , and 20 mg/ml X-Gal. Cells were incubated overnight at  $37^{\circ}\text{C}$  and overlaid with 50% glycerol. Readout was performed optically with light microscopy.

## TZM-bl Luc assay of HEK293T APOBEC3G-expressing cells

A total of 4,000 TZM-bl cells were seeded per well in 96-well plates and incubated overnight. The virus-containing supernatant was serially diluted 1:3 in culture medium and 200  $\mu\text{l}$  of the diluted viral supernatant was added to the cells. Forty-eight post-infection, cells were washed with PBS and lysed using 120  $\mu\text{l}$  of lysis juice (p.j.k.). Plates were incubated for 15 min before a freeze-and-thaw cycle was applied, to ensure complete lysis. Thirty microliters of homogenized lysates were transferred to a white F96 Microwell plate (Nunc) for luminescent readout. One hundred twenty microliters of beetle juice (p.j.k.) was added per well and luminescence was measured

using the GloMax Discover (Promega) with an integration time of 5 s with one reading per well.

## siRNA-based knockdown

If not indicated otherwise, HEK293T cells were transiently transfected with the indicated siRNA at a final concentration of 8 nM using Lipofectamine 2000 (Thermo Scientific) according to the manufacturer's instructions. A further transfection was performed at a final concentration of 12.8 nM of the indicated siRNA to evaluate SRSF1 knockdown efficiency. The following siRNAs were used in this study: Silencer Select Negative Control #2 siRNA (Thermo Scientific) for the negative control siRNA and s12727 (Thermo Scientific) for SRSF1-specific siRNA.

## 4sU tagging

Differentiated THP-1 cells were treated for 30 min with 4sU (Sigma-Aldrich) at a final concentration of 500  $\mu$ M for metabolic labeling of newly transcribed RNA following treatment with IFN $\alpha$ 14 for the indicated amount of time. Labeling, purification, and separation of freshly transcribed RNA was carried out as described elsewhere (110). Newly transcribed RNA concentration and quality was measured using NanoDrop2000c (Thermo Scientific).

## PBMC isolation

PBMCs were isolated from whole blood samples by Ficoll density gradient centrifugation using LeucoSEP tubes (Greiner Bio-One) as described previously (178). RNA of isolated PBMCs was harvested as described above. This study has been approved by the Ethics Committee of the Medical Faculty of the University of Duisburg-Essen (14-6155-BO, 16-7016-BO, and 19-8909-BO). Consent form was not obtained since the data were analyzed anonymously.

## Statistical analysis

Differences between two groups were analyzed by unpaired two-tailed Student's or Welch's *t*-test. Multiple group analyses were performed using one- or two-way ANOVA followed by Bonferroni, Dunnett's, or Tukey's *post-hoc* test. Mixed models followed by Dunnett's *post-hoc* tests were used for time-series analysis of multiple groups. A Kruskal-Wallis test with the Dunn's *post-hoc* multiple comparisons test was applied to compare mRNA levels in PBMCs from acutely and chronically HIV-1-infected patients as well as from healthy donors due to violation of the assumptions for a parametric test. If not

indicated differently, all experiments were repeated in three independent replicates. Asterisks indicated *p*-values as \**p* < 0.05, \*\**p* < 0.01, \*\*\**p* < 0.005, and \*\*\*\**p* < 0.0001.

## Data availability statement

Next-generation sequencing data were deposited in the NCBI Sequence Archive Bioproject with accession PRJNA422935. Further inquiries can be directed to the corresponding author.

## Ethics statement

The studies involving human participants were reviewed and approved by the Ethics Committee of the Medical Faculty of the University of Duisburg-Essen (14-6155-BO, 16-7016-BO, 19-8909-BO). Written informed consent for participation was not required for this study in accordance with the national legislation and the institutional requirements.

## Author contributions

HS: data curation, formal analysis, funding acquisition, investigation, methodology, project administration, visualization, writing-ODP, writing-RE. FR: investigation, writing-RE. AW: methodology, visualization. DH: investigation. BB: investigation. CE: investigation, resources, writing-RE. MS: data curation, investigation. JS: investigation, writing-RE. ZK: investigation. YB: investigation, resources. RS: investigation, resources. SE: resources. KS: funding acquisition, investigation, project administration, resources, writing-RE. UD: conceptualisation, funding acquisition, project administration, resources, supervision, writing-RE. MW: conceptualisation, funding acquisition, methodology, project administration, resources, supervision, visualization writing-ODP, writing-RE. All authors contributed to the article and approved the submitted version.

## Funding

These studies were funded by the DFG (WI 5086/1-1; SU1030/1-2), the Jürgen-Manchot-Stiftung (HS and MW), the Hessian Ministry of Higher Education, Research and the Arts (TheraNova, MW), and the Medical Faculty of the University of Duisburg-Essen (HS and KS). The authors thank the Jürgen-Manchot-Stiftung for the doctoral fellowship of Helene Sertznig.

## Acknowledgments

We thank Christiane Pallas for excellent technical assistance. We thank Heiner Schaal for providing plasmid



DNA and Mirko Trilling for fruitful discussions. The following reagents were obtained through the AIDS Research and Reference Reagent Program, Division of AIDS, NIAID, NIH: TZM-bl cells from Dr. John C. Kappes and Dr. Xiaoyun Wu. pEGFP-SF2 (179) was a gift from Tom Misteli (Addgene plasmid # 17990; <http://n2t.net/addgene:17990>; RRID: Addgene\_17990). pcDNA-FLAG-SF2 was a gift from Honglin Chen (Addgene plasmid # 99021; <http://n2t.net/addgene:99021>; RRID: Addgene\_99021) (117).

## Conflict of interest

The authors declare that the research was conducted in the absence of any commercial or financial relationships that could be construed as a potential conflict of interest.

## References

- Katze MG, He Y, Gale M Jr. Viruses and interferon: a fight for supremacy. *Nat Rev Immunol* (2002) 2(9):675–87. doi: 10.1038/nri888
- Lee AJ, Ashkar AA. The dual nature of type I and type II interferons. *Front Immunol* (2018) 9:2061. doi: 10.3389/fimmu.2018.02061
- Iwasaki A. A virological view of innate immune recognition. *Annu Rev Microbiol* (2012) 66:177–96. doi: 10.1146/annurev-micro-092611-150203
- Mogensen TH. Pathogen recognition and inflammatory signaling in innate immune defenses. *Clin Microbiol Rev* (2009) 22(2):240–73. doi: 10.1128/CMR.00046-08
- Gao D, Wu J, Wu YT, Du F, Aroh C, Yan N, et al. Cyclic GMP-AMP synthase is an innate immune sensor of HIV and other retroviruses. *Science* (2013) 341(6148):903–6. doi: 10.1126/science.1240933
- Ivashkiv LB, Donlin LT. Regulation of type I interferon responses. *Nat Rev Immunol* (2014) 14(1):36–49. doi: 10.1038/nri3581
- Hervas-Stubbs S, Perez-Gracia JL, Rouzaut A, Sanmamed MF, Le Bon A, Melero I. Direct effects of type I interferons on cells of the immune system. *Clin Cancer Res* (2011) 17(9):2619–27. doi: 10.1158/1078-0432.CCR-10-1114
- Platanias LC. Mechanisms of type-I- and type-II-interferon-mediated signalling. *Nat Rev Immunol* (2005) 5(5):375–86. doi: 10.1038/nri1604
- Perng YC, Lenschow DJ. ISG15 in antiviral immunity and beyond. *Nat Rev Microbiol* (2018) 16(7):423–39. doi: 10.1038/s41579-018-0020-5
- Morales DJ, Lenschow DJ. The antiviral activities of ISG15. *J Mol Biol* (2013) 425(24):4995–5008. doi: 10.1016/j.jmb.2013.09.041
- Pincetic A, Kuang Z, Seo EJ, Leis J. The interferon-induced gene ISG15 blocks retrovirus release from cells late in the budding process. *J virol* (2010) 84(9):4725–36. doi: 10.1128/JVI.02478-09
- Refsland EW, Harris RS. The APOBEC3 family of retroelement restriction factors. *Curr topics Microbiol Immunol* (2013) 371:1–27. doi: 10.1007/978-3-642-37765-5\_1
- Wissing S, Galloway NL, Greene WC. HIV-1 vif versus the APOBEC3 cytidine deaminases: an intracellular duel between pathogen and host restriction factors. *Mol aspects Med* (2010) 31(5):383–97. doi: 10.1016/j.mam.2010.06.001
- Neil SJ, Zang T, Bieniasz PD. Tetherin inhibits retrovirus release and is antagonized by HIV-1 vpu. *Nature* (2008) 451(7177):425–30. doi: 10.1038/nature06553
- Perez-Caballero D, Zang T, Ebrahimi A, McNatt MW, Gregory DA, Johnson MC, et al. Tetherin inhibits HIV-1 release by directly tethering virions to cells. *Cell* (2009) 139(3):499–511. doi: 10.1016/j.cell.2009.08.039
- Goujon C, Moncorge O, Bauby H, Doyle T, Ward CC, Schaller T, et al. Human MX2 is an interferon-induced post-entry inhibitor of HIV-1 infection. *Nature* (2013) 502(7472):559–62. doi: 10.1038/nature12542
- Kane M, Yadav SS, Bitzegeio J, Kutluay SB, Zang T, Wilson SJ, et al. MX2 is an interferon-induced inhibitor of HIV-1 infection. *Nature* (2013) 502(7472):563–6. doi: 10.1038/nature12653
- Hrecka K, Hao C, Gierszewska M, Swanson SK, Kesik-Brodacka M, Srivastava S, et al. Vpx relieves inhibition of HIV-1 infection of macrophages mediated by the SAMHD1 protein. *Nature* (2011) 474(7353):658–61. doi: 10.1038/nature10195
- Laguette N, Sobhian B, Casartelli N, Ringard M, Chable-Bessia C, Segal E, et al. SAMHD1 is the dendritic- and myeloid-cell-specific HIV-1 restriction factor counteracted by vpx. *Nature* (2011) 474(7353):654–7. doi: 10.1038/nature10117
- Lahouassa H, Daddacha W, Hofmann H, Ayinde D, Logue EC, Dragin L, et al. SAMHD1 restricts the replication of human immunodeficiency virus type 1 by depleting the intracellular pool of deoxynucleoside triphosphates. *Nat Immunol* (2012) 13(3):223–8. doi: 10.1038/ni.2236
- Lee WJ, Fu RM, Liang C, Sloan RD. IFITM proteins inhibit HIV-1 protein synthesis. *Sci Rep* (2018) 8(1):14551. doi: 10.1038/s41598-018-32785-5
- Lu J, Pan Q, Rong L, He W, Liu SL, Liang C. The IFITM proteins inhibit HIV-1 infection. *J virol* (2011) 85(5):2126–37. doi: 10.1128/JVI.01531-10
- Li Y, Sun B, Esser S, Jessen H, Streeck H, Widera M, et al. Expression pattern of individual IFNA subtypes in chronic HIV infection. *J Interferon Cytokine Res* (2017) 37(12):541–9. doi: 10.1089/jir.2017.0076
- Li SF, Gong MJ, Zhao FR, Shao JJ, Xie YL, Zhang YG, et al. Type I interferons: Distinct biological activities and current applications for viral infection. *Cell Physiol Biochem* (2018) 51(5):2377–96. doi: 10.1159/000495897
- Gibbert K, Schlaak JF, Yang D, Dittmer U. IFN-alpha subtypes: distinct biological activities in anti-viral therapy. *Br J Pharmacol* (2013) 168(5):1048–58. doi: 10.1111/bph.12010
- Harper MS, Guo K, Gibbert K, Lee EJ, Dillon SM, Barrett BS, et al. Interferon-alpha subtypes in an ex vivo model of acute HIV-1 infection: Expression, potency and effector mechanisms. *PLoS pathogens* (2015) 11(11):e1005254. doi: 10.1371/journal.ppat.1005254
- Lavender KJ, Gibbert K, Peterson KE, Van Dis E, Francois S, Woods T, et al. Interferon alpha subtype-specific suppression of HIV-1 infection in vivo. *J Virol* (2016) 90(13):6001–13. doi: 10.1128/JVI.00451-16
- Antonelli G, Scagnolari C, Moschella F, Proietti E. Twenty-five years of type I interferon-based treatment: a critical analysis of its therapeutic use. *Cytokine Growth Factor Rev* (2015) 26(2):121–31. doi: 10.1016/j.cytogfr.2014.12.006
- Megger DA, Philipp J, Le-Trilling VTK, Sitek B, Trilling M. Deciphering of the human interferon-regulated proteome by mass spectrometry-based quantitative analysis reveals extent and dynamics of protein induction and repression. *Front Immunol* (2017) 8:1139. doi: 10.3389/fimmu.2017.01139
- Trilling M, Bellora N, Rutkowski AJ, de Graaf M, Dickinson P, Robertson K, et al. Deciphering the modulation of gene expression by type I and II interferons

## Publisher's note

All claims expressed in this article are solely those of the authors and do not necessarily represent those of their affiliated organizations, or those of the publisher, the editors and the reviewers. Any product that may be evaluated in this article, or claim that may be made by its manufacturer, is not guaranteed or endorsed by the publisher.

## Supplementary material

The Supplementary Material for this article can be found online at: <https://www.frontiersin.org/articles/10.3389/fimmu.2022.935800/full#supplementary-material>



- combining 4sU-tagging, translational arrest and in silico promoter analysis. *Nucleic Acids Res* (2013) 41(17):8107–25. doi: 10.1093/nar/gkt589
31. Bushman FD, Malani N, Fernandes J, D'Orso I, Cagney G, Diamond TL, et al. Host cell factors in HIV replication: meta-analysis of genome-wide studies. *PLoS pathogens* (2009) 5(5):e1000437. doi: 10.1371/journal.ppat.1000437
  32. Roebuck KA, Saifuddin M. Regulation of HIV-1 transcription. *Gene expression* (1999) 8(2):67–84.
  33. Wu Y. HIV-1 gene expression: lessons from provirus and non-integrated DNA. *Retrovirology* (2004) 1:13. doi: 10.1186/1742-4690-1-13
  34. Stoltzfus CM. Chapter 1. regulation of HIV-1 alternative RNA splicing and its role in virus replication. *Adv Virus Res* (2009) 74:1–40. doi: 10.1016/S0065-3527(09)74001-1
  35. Sertznig H, Hillebrand F, Erkelenz S, Schaal H, Widera M. Behind the scenes of HIV-1 replication: Alternative splicing as the dependency factor on the quiet. *Virology* (2018) 516:176–88. doi: 10.1016/j.virol.2018.01.011
  36. Purcell DF, Martin MA. Alternative splicing of human immunodeficiency virus type 1 mRNA modulates viral protein expression, replication, and infectivity. *J virol* (1993) 67(11):6365–78. doi: 10.1128/jvi.67.11.6365-6378.1993
  37. Karn J, Stoltzfus CM. Transcriptional and posttranscriptional regulation of HIV-1 gene expression. *Cold Spring Harbor Perspect Med* (2012) 2(2):a006916. doi: 10.1101/cshperspect.a006916
  38. Baralle M, Baralle FE. The splicing code. *Biosystems* (2018) 164:39–48. doi: 10.1016/j.biosystems.2017.11.002
  39. Wang Z, Burge CB. Splicing regulation: from a parts list of regulatory elements to an integrated splicing code. *RNA* (2008) 14(5):802–13. doi: 10.1261/rna.876308
  40. Barash Y, Calarco JA, Gao W, Pan Q, Wang X, Shai O, et al. Deciphering the splicing code. *Nature* (2010) 465(7294):53–9. doi: 10.1038/nature09000
  41. Geuens T, Bouhy D, Timmerman V. The hnRNP family: insights into their role in health and disease. *Hum Genet* (2016) 135(8):851–67. doi: 10.1007/s00439-016-1683-5
  42. Manley JL, Tacke R. SR proteins and splicing control. *Genes Dev* (1996) 10(13):1569–79. doi: 10.1101/gad.10.13.1569
  43. Brass AL, Dykxhoorn DM, Benita Y, Yan N, Engelman A, Xavier RJ, et al. Identification of host proteins required for HIV infection through a functional genomic screen. *Science* (2008) 319(5865):921–6. doi: 10.1126/science.1152725
  44. König R, Zhou Y, Elleder D, Diamond TL, Bonamy GM, Irelan JT, et al. Global analysis of host-pathogen interactions that regulate early-stage HIV-1 replication. *Cell* (2008) 135(1):49–60. doi: 10.1016/j.cell.2008.07.032
  45. Fu C, Yang S, Yang X, Lian X, Huang Y, Dong X, et al. Human gene functional network-informed prediction of HIV-1 host dependency factors. *mSystems* (2020) 5(6):e00960-20. doi: 10.1128/mSystems.00960-20
  46. Zhou H, Xu M, Huang Q, Gates AT, Zhang XD, Castle JC, et al. Genome-scale RNAi screen for host factors required for HIV replication. *Cell Host Microbe* (2008) 4(5):495–504. doi: 10.1016/j.chom.2008.10.004
  47. Zhu J, Davoli T, Perriera JM, Chin CR, Gaiha GD, John SP, et al. Comprehensive identification of host modulators of HIV-1 replication using multiple orthologous RNAi reagents. *Cell Rep* (2014) 9(2):752–66. doi: 10.1016/j.celrep.2014.09.031
  48. Anko ML. Regulation of gene expression programmes by serine-arginine rich splicing factors. *Semin Cell Dev Biol* (2014) 32:11–21. doi: 10.1016/j.semcdb.2014.03.011
  49. Bourgeois CF, Lejeune F, Stevenin J. Broad specificity of SR (serine/arginine) proteins in the regulation of alternative splicing of pre-messenger RNA. *Prog Nucleic Acid Res Mol Biol* (2004) 78:37–88. doi: 10.1016/S0079-6603(04)78002-2
  50. Fu XD. The superfamily of arginine/serine-rich splicing factors. *RNA* (1995) 1(7):663–80.
  51. Graveley BR. Sorting out the complexity of SR protein functions. *RNA* (2000) 6(9):1197–211. doi: 10.1017/S135583820000960
  52. Jeong S. SR proteins: Binders, regulators, and connectors of RNA. *Molecules Cells* (2017) 40(1):1–9. doi: 10.14348/molcells.2017.2319
  53. Matera AG, Wang Z. A day in the life of the spliceosome. *Nat Rev Mol Cell Biol* (2014) 15(2):108–21. doi: 10.1038/nrm3742
  54. Shepard PJ, Hertel KJ. The SR protein family. *Genome Biol* (2009) 10(10):242. doi: 10.1186/gb-2009-10-10-242
  55. Kannan N, Neuwald AF. Evolutionary constraints associated with functional specificity of the CMGC protein kinases MAPK, CDK, GSK, SRPK, DYRK, and CK2alpha. *Protein Sci Publ Protein Society* (2004) 13(8):2059–77. doi: 10.1110/ps.04637904
  56. Choudhary C, Kumar C, Gnad F, Nielsen ML, Rehman M, Walther TC, et al. Lysine acetylation targets protein complexes and co-regulates major cellular functions. *Science* (2009) 325(5942):834–40. doi: 10.1126/science.1175371
  57. Liu Q, Dreyfuss G. *In vivo* and *in vitro* arginine methylation of RNA-binding proteins. *Mol Cell Biol* (1995) 15(5):2800–8. doi: 10.1128/MCB.15.5.2800
  58. Siebel CW, Guthrie C. The essential yeast RNA binding protein Np13p is methylated. *Proc Natl Acad Sci U S A* (1996) 93(24):13641–6. doi: 10.1073/pnas.93.24.13641
  59. Yun CY, Fu XD. Conserved SR protein kinase functions in nuclear import and its action is counteracted by arginine methylation in *Saccharomyces cerevisiae*. *J Cell Biol* (2000) 150(4):707–18. doi: 10.1083/jcb.150.4.707
  60. Cho S, Hoang A, Sinha R, Zhong XY, Fu XD, Krainer AR, et al. Interaction between the RNA binding domains of ser-arg splicing factor 1 and U1-70K snRNP protein determines early spliceosome assembly. *Proc Natl Acad Sci U S A* (2011) 108(20):8233–8. doi: 10.1073/pnas.1017700108
  61. Erkelenz S, Mueller WF, Evans MS, Busch A, Schoneweis K, Hertel KJ, et al. Position-dependent splicing activation and repression by SR and hnRNP proteins rely on common mechanisms. *RNA* (2013) 19(1):96–102. doi: 10.1261/rna.037044.112
  62. Fu XD, Maniatis T. The 35-kDa mammalian splicing factor SC35 mediates specific interactions between U1 and U2 small nuclear ribonucleoprotein particles at the 3' splice site. *Proc Natl Acad Sci U S A* (1992) 89(5):1725–9. doi: 10.1073/pnas.89.5.1725
  63. Lin S, Fu XD. SR proteins and related factors in alternative splicing. *Adv Exp Med Biol* (2007) 623:107–22. doi: 10.1007/978-0-387-77374-2\_7
  64. Hicks MJ, Mueller WF, Shepard PJ, Hertel KJ. Competing upstream 5' splice sites enhance the rate of proximal splicing. *Mol Cell Biol* (2010) 30(8):1878–86. doi: 10.1128/MCB.01071-09
  65. Ibrahim EC, Schaal TD, Hertel KJ, Reed R, Maniatis T. Serine/arginine-rich protein-dependent suppression of exon skipping by exonic splicing enhancers. *Proc Natl Acad Sci U S A* (2005) 102(14):5002–7. doi: 10.1073/pnas.0500543102
  66. Kanopka A, Muhlemann O, Akusjarvi G. Inhibition by SR proteins of splicing of a regulated adenovirus pre-mRNA. *Nature* (1996) 381(6582):535–8. doi: 10.1038/381535a0
  67. Ji X, Zhou Y, Pandit S, Huang J, Li H, Lin CY, et al. SR proteins collaborate with 7SK and promoter-associated nascent RNA to release paused polymerase. *Cell* (2013) 153(4):855–68. doi: 10.1016/j.cell.2013.04.028
  68. Sapra AK, Anko ML, Grishina I, Lorenz M, Pabis M, Poser I, et al. SR protein family members display diverse activities in the formation of nascent and mature mRNPs in vivo. *Mol Cell* (2009) 34(2):179–90. doi: 10.1016/j.molcel.2009.02.031
  69. Huang Y, Gattoni R, Stevenin J, Steitz JA. SR splicing factors serve as adapter proteins for TAP-dependent mRNA export. *Mol Cell* (2003) 11(3):837–43. doi: 10.1016/S1097-2765(03)00089-3
  70. Huang Y, Steitz JA. Splicing factors SRp20 and 9G8 promote the nucleocytoplasmic export of mRNA. *Mol Cell* (2001) 7(4):899–905. doi: 10.1016/S1097-2765(01)00233-7
  71. Huang Y, Steitz JA. SRproteins along a messenger's journey. *Mol Cell* (2005) 17(5):613–5. doi: 10.1016/j.molcel.2005.02.020
  72. Popp MW, Maquat LE. The dharma of nonsense-mediated mRNA decay in mammalian cells. *Molecules Cells* (2014) 37(1):1–8. doi: 10.14348/molcells.2014.2193
  73. Manley JL, Krainer AR. A rational nomenclature for serine/arginine-rich protein splicing factors (SR proteins). *Genes Dev* (2010) 24(11):1073–4. doi: 10.1101/gad.1934910
  74. Krainer AR, Conway GC, Kozak D. The essential pre-mRNA splicing factor SF2 influences 5' splice site selection by activating proximal sites. *Cell* (1990) 62(1):35–42. doi: 10.1016/0092-8674(90)90237-9
  75. Ge H, Manley JL. A protein factor, ASF, controls cell-specific alternative splicing of SV40 early pre-mRNA *in vitro*. *Cell* (1990) 62(1):25–34. doi: 10.1016/0092-8674(90)90236-8
  76. Chang B, Levin J, Thompson WA, Fairbrother WG. High-throughput binding analysis determines the binding specificity of ASF/SF2 on alternatively spliced human pre-mRNAs. *Comb Chem High Throughput Screen* (2010) 13(3):242–52. doi: 10.2174/138620710790980522
  77. Das S, Krainer AR. Emerging functions of SRSF1, splicing factor and oncoprotein, in RNA metabolism and cancer. *Mol Cancer Res MCR* (2014) 12(9):1195–204. doi: 10.1158/1541-7786.MCR-14-0131
  78. Caputi M, Freund M, Kammler S, Asang C, Schaal H. A bidirectional SF2/ASF- and SRp40-dependent splicing enhancer regulates human immunodeficiency virus type 1 rev, env, vpu, and nef gene expression. *J virol* (2004) 78(12):6517–26. doi: 10.1128/JVI.78.12.6517-6526.2004
  79. Kammler S, Otte M, Hauber I, Kjems J, Hauber J, Schaal H. The strength of the HIV-1 3' splice sites affects rev function. *Retrovirology* (2006) 3:89. doi: 10.1186/1742-4690-3-89
  80. Staffa A, Cochrane A. Identification of positive and negative splicing regulatory elements within the terminal tat-rev exon of human

- immunodeficiency virus type 1. *Mol Cell Biol* (1995) 15(8):4597–605. doi: 10.1128/MCB.15.8.4597
81. Tange TO, Kjems J. SF2/ASF binds to a splicing enhancer in the third HIV-1 tat exon and stimulates U2AF binding independently of the RS domain. *J Mol Biol* (2001) 312(4):649–62. doi: 10.1006/jmbi.2001.4971
82. Paz S, Caputi M. SRSF1 inhibition of HIV-1 gene expression. *Oncotarget* (2015) 6(23):19362–3. doi: 10.18632/oncotarget.5125
83. Paz S, Krainer AR, Caputi M. HIV-1 transcription is regulated by splicing factor SRSF1. *Nucleic Acids Res* (2014) 42(22):13812–23. doi: 10.1093/nar/gku1170
84. Jablonski JA, Caputi M. Role of cellular RNA processing factors in human immunodeficiency virus type 1 mRNA metabolism, replication, and infectivity. *J virol* (2009) 83(2):981–92. doi: 10.1128/JVI.01801-08
85. Ropers D, Ayadi L, Gattori R, Jacquenet S, Damier L, Branlant C, et al. Differential effects of the SR proteins 9G8, SC35, ASF/SF2, and SRp40 on the utilization of the A1 to A5 splicing sites of HIV-1 RNA. *J Biol Chem* (2004) 279(29):29963–73. doi: 10.1074/jbc.M404452200
86. Jacquenet S, Decimo D, Muriaux D, Darlix JL. Dual effect of the SR proteins ASF/SF2, SC35 and 9G8 on HIV-1 RNA splicing and virion production. *Retrovirology* (2005) 2:33. doi: 10.1186/1742-4690-2-33
87. Dillon SM, Guo K, Austin GL, Gianella S, Engen PA, Mutlu EA, et al. A compartmentalized type I interferon response in the gut during chronic HIV-1 infection is associated with immunopathogenesis. *AIDS* (2018) 32(12):1599–611. doi: 10.1097/QAD.0000000000001863
88. Fiebig EW, Wright DJ, Rawal BD, Garrett PE, Schumacher RT, Peddada L, et al. Dynamics of HIV viremia and antibody seroconversion in plasma donors: implications for diagnosis and staging of primary HIV infection. *AIDS* (2003) 17(13):1871–9. doi: 10.1097/00002030-200309050-00005
89. Lourenco L, Colley G, Nosyk B, Shopin D, Montaner JS, Lima VD, et al. High levels of heterogeneity in the HIV cascade of care across different population subgroups in British Columbia, Canada. *PLoS One* (2014) 9(12):e115277. doi: 10.1371/journal.pone.0115277
90. Pereyra F, Addo MM, Kaufmann DE, Liu Y, Miura T, Rathod A, et al. Genetic and immunologic heterogeneity among persons who control HIV infection in the absence of therapy. *J Infect diseases* (2008) 197(4):563–71. doi: 10.1086/526786
91. Gibbert K, Dittmer U. Distinct antiviral activities of IFN- $\alpha$  subtypes. *Immunotherapy* (2011) 3(7):813–6. doi: 10.2217/imt.11.74
92. Hardy MP, Owczarek CM, Jermini LS, Ejdebäck M, Hertzog PJ. Characterization of the type I interferon locus and identification of novel genes. *Genomics* (2004) 84(2):331–45. doi: 10.1016/j.ygeno.2004.03.003
93. Le-Trilling VTK, Wohlgemuth K, Ruckborn MU, Jagnjic A, Maaßen F, Timmer L, et al. STAT2-dependent immune responses ensure host survival despite the presence of a potent viral antagonist. *J Virol* (2018) 92(14):e00296-18. doi: 10.1128/JVI.00296-18
94. Escher TE, Lui AJ, Geanes ES, Walter KR, Tawfik O, Hagan CR, et al. Interaction between MUC1 and STAT1 drives IFITM1 overexpression in aromatase inhibitor-resistant breast cancer cells and mediates estrogen-induced apoptosis. *Mol Cancer Res MCR* (2019) 17(5):1180–94. doi: 10.1158/1541-7786.MCR-18-0916
95. Widera M, Hillebrand F, Erkelenz S, Vasudevan A, Munk C, Schaal H. A functional conserved intronic G run in HIV-1 intron 3 is critical to counteract APOBEC3G-mediated host restriction. *Retrovirology* (2014) 11(1):72. doi: 10.1186/s12977-014-0072-1
96. Mohammadi P, Desfarges S, Bartha I, Joos B, Zangger N, Munoz M, et al. 24 hours in the life of HIV-1 in a T cell line. *PLoS pathogens* (2013) 9(1):e1003161. doi: 10.1371/journal.ppat.1003161
97. Zahoor MA, Xue G, Sato H, Aida Y. Genome-wide transcriptional profiling reveals that HIV-1 vpr differentially regulates interferon-stimulated genes in human monocyte-derived dendritic cells. *Virus Res* (2015) 208:156–63. doi: 10.1016/j.virusres.2015.06.017
98. Zahoor MA, Xue G, Sato H, Murakami T, Takeshima SN, Aida Y. HIV-1 vpr induces interferon-stimulated genes in human monocyte-derived macrophages. *PLoS One* (2014) 9(8):e106418. doi: 10.1371/journal.pone.0106418
99. Kukkonen S, Martinez-Viedma Mdel P, Kim N, Manrique M, Aldovini A. HIV-1 tat second exon limits the extent of tat-mediated modulation of interferon-stimulated genes in antigen presenting cells. *Retrovirology* (2014) 11:30. doi: 10.1186/1742-4690-11-30
100. Ellegard R, Crisci E, Burgener A, Sjowall C, Birse K, Westmacott G, et al. Complement opsonization of HIV-1 results in decreased antiviral and inflammatory responses in immature dendritic cells via CR3. *J Immunol* (2014) 193(9):4590–601. doi: 10.4049/jimmunol.1401781
101. Doehle BP, Chang K, Fleming L, McNeven J, Hladik F, McElrath MJ, et al. Vpu-deficient HIV strains stimulate innate immune signaling responses in target cells. *J virol* (2012) 86(16):8499–506. doi: 10.1128/JVI.00424-12
102. Pestka S, Krause CD, Walter MR. Interferons, interferon-like cytokines, and their receptors. *Immunol Rev* (2004) 202:8–32. doi: 10.1111/j.0105-2896.2004.00204.x
103. Wheelock EF. Interferon-like virus-inhibitor induced in human leukocytes by phytohemagglutinin. *Science* (1965) 149(3681):310–1. doi: 10.1126/science.149.3681.310
104. Bhat MY, Solanki HS, Advani J, Khan AA, Keshava Prasad TS, Gowda H, et al. Comprehensive network map of interferon gamma signaling. *J Cell Commun Signal* (2018) 12(4):745–51. doi: 10.1007/s12079-018-0486-y
105. Pine I R, Decker T, Kessler DS, Levy DE, Darnell JE Jr. Purification and cloning of interferon-stimulated gene factor 2 (ISGF2): ISGF2 (IRF-1) can bind to the promoters of both beta interferon- and interferon-stimulated genes but is not a primary transcriptional activator of either. *Mol Cell Biol* (1990) 10(6):2448–57. doi: 10.1128/mcb.10.6.2448-2457.1990
106. Carlin AF, Plummer EM, Vizcarra EA, Sheets N, Joo Y, Tang W, et al. An IRF-3-, IRF-5-, and IRF-7-Independent pathway of dengue viral resistance utilizes IRF-1 to stimulate type I and II interferon responses. *Cell Rep* (2017) 21(6):1600–12. doi: 10.1016/j.celrep.2017.10.054
107. Melvin WT, Milne HB, Slater AA, Allen HJ, Keir HM. Incorporation of 6-thioguanosine and 4-thiouridine into RNA. Application to isolation of newly synthesized RNA by affinity chromatography. *Eur J Biochem* (1978) 92(2):373–9. doi: 10.1111/j.1432-1033.1978.tb12756.x
108. Rädle B, Rutkowski AJ, Ruzsics Z, Friedel CC, Koszinowski UH, Dölken L. Metabolic labeling of newly transcribed RNA for high resolution gene expression profiling of RNA synthesis, processing and decay in cell culture. *J Visualized Experiments* (2013) 78. doi: 10.3791/50195
109. Windhager L, Bonfert T, Burger K, Ruzsics Z, Krebs S, Kaufmann S, et al. Ultrashort and progressive 4sU-tagging reveals key characteristics of RNA processing at nucleotide resolution. *Genome Res* (2012) 22(10):2031–42. doi: 10.1101/gr.131847.111
110. Garibaldi A, Carranza F, Hertel KJ. Isolation of newly transcribed RNA using the metabolic label 4-thiouridine. *Methods Mol Biol* (2017) 1648:169–76. doi: 10.1007/978-1-4939-7204-3\_13
111. Polzer S, van Yperen M, Kirst M, Schwalbe B, Schaal H, Schreiber M. Neutralization of X4- and R5-tropic HIV-1 NL4-3 variants by HOCl-modified serum albumins. *BMC Res notes* (2010) 3:155. doi: 10.1186/1756-0500-3-155
112. Akari H, Fujita M, Kao S, Khan MA, Shehu-Xhilaga M, Adachi A, et al. High level expression of human immunodeficiency virus type-1 vif inhibits viral infectivity by modulating proteolytic processing of the gag precursor at the p2/nucleocapsid processing site. *J Biol Chem* (2004) 279(13):12355–62. doi: 10.1074/jbc.M312426200
113. Mandal D, Feng Z, Stoltzfus CM. Excessive RNA splicing and inhibition of HIV-1 replication induced by modified U1 small nuclear RNAs. *J virol* (2010) 84(24):12790–800. doi: 10.1128/JVI.01257-10
114. Widera M, Erkelenz S, Hillebrand F, Krikoni A, Widera D, Kaisers W, et al. An intronic G run within HIV-1 intron 2 is critical for splicing regulation of vif mRNA. *J virol* (2013) 87(5):2707–20. doi: 10.1128/JVI.02755-12
115. Adachi A, Gendelman HE, Koenig S, Folks T, Willey R, Rabson A, et al. Production of acquired immunodeficiency syndrome-associated retrovirus in human and nonhuman cells transfected with an infectious molecular clone. *J virol* (1986) 59(2):284–91. doi: 10.1128/jvi.59.2.284-291.1986
116. Wei X, Decker JM, Liu H, Zhang Z, Arani RB, Kilby JM, et al. Emergence of resistant human immunodeficiency virus type 1 in patients receiving fusion inhibitor (T-20) monotherapy. *Antimicrobial Agents chemother* (2002) 46(6):1896–905. doi: 10.1128/AAC.46.6.1896-1905.2002
117. Huang YQ, Ling XH, Yuan RQ, Chen ZY, Yang SB, Huang HX, et al. miR30c suppresses prostate cancer survival by targeting the ASF/SF2 splicing factor oncoprotein. *Mol Med Rep* (2017) 16(3):2431–8. doi: 10.3892/mmr.2017.6910
118. Massanella M, Singhania A, Beliakova-Bethell N, Pier R, Lada SM, White CH, et al. Differential gene expression in HIV-infected individuals following ART. *Antiviral Res* (2013) 100(2):420–8. doi: 10.1016/j.antiviral.2013.07.017
119. Baltimore D. Expression of animal virus genomes. *Bacteriol Rev* (1971) 35(3):235–41. doi: 10.1128/br.35.3.235-241.1971
120. Booth JS, Toapanta FR, Salerno-Goncalves R, Patil S, Kader HA, Safta AM, et al. Characterization and functional properties of gastric tissue-resident memory T cells from children, adults, and the elderly. *Front Immunol* (2014) 5:294. doi: 10.3389/fimmu.2014.00294
121. Goll R, Husebekk A, Isaksen V, Kauric G, Hansen T, Florholmen J. Increased frequency of antral CD4 T and CD19 b cells in patients with helicobacter pylori-related peptic ulcer disease. *Scandinavian J Immunol* (2005) 61(1):92–7. doi: 10.1111/j.0300-9475.2005.01537.x
122. Satoh Y, Ogawara H, Kawamura O, Kusano M, Murakami H. Clinical significance of peripheral blood T lymphocyte subsets in helicobacter pylori-infected patients. *Gastroenterol Res Pract* (2012) 2012:819842. doi: 10.1155/2012/819842

123. Trejdosiewicz LK, Badr-el-Din S, Smart CJ, Malizia G, Oakes DJ, Heatley RV, et al. Colonic mucosal T lymphocytes in ulcerative colitis: expression of CD7 antigen in relation to MHC class II (HLA-d) antigens. *Digestive Dis Sci* (1989) 34(9):1449–56. doi: 10.1007/BF01538084
124. Trejdosiewicz LK, Smart CJ, Oakes DJ, Howdle PD, Malizia G, Campana D, et al. Expression of T-cell receptors TcR1 (gamma/delta) and TcR2 (alpha/beta) in the human intestinal mucosa. *Immunology* (1989) 68(1):7–12.
125. Goode T, O'Connell J, Ho WZ, O'Sullivan GC, Collins JK, Douglas SD, et al. Differential expression of neurokinin-1 receptor by human mucosal and peripheral lymphoid cells. *Clin Diagn Lab Immunol* (2000) 7(3):371–6. doi: 10.1128/CDL117.3.371-376.2000
126. Smythies LE, Sellers M, Clements RH, Mosteller-Barnum M, Meng G, Benjamin WH, et al. Human intestinal macrophages display profound inflammatory anergy despite avid phagocytic and bacteriocidal activity. *J Clin Invest* (2005) 115(1):66–75. doi: 10.1172/JCI200519229
127. Smart I CJ, Trejdosiewicz LK, Badr-el-Din S, Heatley RV. T Lymphocytes of the human colonic mucosa: functional and phenotypic analysis. *Clin Exp Immunol* (1988) 73(1):63–9.
128. Ertel A, Verghese A, Byers SW, Ochs M, Tozeren A. Pathway-specific differences between tumor cell lines and normal and tumor tissue cells. *Mol cancer* (2006) 5(1):55. doi: 10.1186/1476-4598-5-55
129. Pan C, Kumar C, Bohl S, Klingmueller U, Mann M. Comparative proteomic phenotyping of cell lines and primary cells to assess preservation of cell type-specific functions. *Mol Cell Proteomics MCP* (2009) 8(3):443–50. doi: 10.1074/mcp.M800258-MCP200
130. Crisler WJ, Lenz LL. Crosstalk between type I and II interferons in regulation of myeloid cell responses during bacterial infection. *Curr Opin Immunol* (2018) 54:35–41. doi: 10.1016/j.coi.2018.05.014
131. Gough DJ, Messina NL, Hii L, Gould JA, Sabapathy K, Robertson AP, et al. Functional crosstalk between type I and II interferon through the regulated expression of STAT1. *PLoS Biol* (2010) 8(4):e1000361. doi: 10.1371/journal.pbio.1000361
132. Takaoka A, Mitani Y, Suemori H, Sato M, Yokochi T, Noguchi S, et al. Cross talk between interferon-gamma and -alpha/beta signaling components in caveolar membrane domains. *Science* (2000) 288(5475):2357–60. doi: 10.1126/science.288.5475.2357
133. Das S, Anczukow O, Akerman M, Krainer AR. Oncogenic splicing factor SRSF1 is a critical transcriptional target of MYC. *Cell Rep* (2012) 1(2):110–7. doi: 10.1016/j.celrep.2011.12.001
134. Mao DY, Watson JD, Yan PS, Baryste-Lovejoy D, Khosravi F, Wong WW, et al. Analysis of myc bound loci identified by CpG island arrays shows that max is essential for myc-dependent repression. *Curr Biol CB* (2003) 13(10):882–6. doi: 10.1016/S0960-9822(03)00297-5
135. Einat M, Resnitzky D, Kimchi A. Close link between reduction of c-myc expression by interferon and, G0/G1 arrest. *Nature* (1985) 313(6003):597–600. doi: 10.1038/313597a0
136. Chatterjee D, Savarese TM. Posttranscriptional regulation of c-myc proto-oncogene expression and growth inhibition by recombinant human interferon-beta ser17 in a human colon carcinoma cell line. *Cancer Chemother Pharmacol* (1992) 30(1):12–20. doi: 10.1007/BF00686479
137. Dani C, Mechti N, Piechaczyk M, Lebleu B, Jeanteur P, Blanchard JM. Increased rate of degradation of c-myc mRNA in interferon-treated daudi cells. *Proc Natl Acad Sci U S A* (1985) 82(15):4896–9. doi: 10.1073/pnas.82.15.4896
138. Ding F, Su CJ, Edmonds KK, Liang G, Elowitz MB. Dynamics and functional roles of splicing factor autoregulation. *Cell Reports* (2022) 39(12):110985. doi: 10.1016/j.celrep.2022.110985
139. Sun S, Zhang Z, Sinha R, Karni R, Krainer AR. SF2/ASF autoregulation involves multiple layers of post-transcriptional and translational control. *Nat Struct Mol Biol* (2010) 17(3):306–12. doi: 10.1038/nsmb.1750
140. Fregoso OI, Das S, Akerman M, Krainer AR. Splicing-factor oncoprotein SRSF1 stabilizes p53 via RPL5 and induces cellular senescence. *Mol Cell* (2013) 50(1):56–66. doi: 10.1016/j.molcel.2013.02.001
141. Karni R, de Stanchina E, Lowe SW, Sinha R, Mu D, Krainer AR. The gene encoding the splicing factor SF2/ASF is a proto-oncogene. *Nat Struct Mol Biol* (2007) 14(3):185–93. doi: 10.1038/nsmb1209
142. Goncalves V, Jordan P. Posttranscriptional regulation of splicing factor SRSF1 and its role in cancer cell biology. *BioMed Res Int* (2015) 2015:287048. doi: 10.1155/2015/287048
143. Zhou Z, Fu XD. Regulation of splicing by SR proteins and SR protein-specific kinases. *Chromosoma* (2013) 122(3):191–207. doi: 10.1007/s00412-013-0407-z
144. Erkelenz S, Poschmann G, Theiss S, Stefanski A, Hillebrand F, Otte M, et al. Tra2-mediated recognition of HIV-1 5' splice site D3 as a key factor in the processing of vpr mRNA. *J virol* (2013) 87(5):2721–34. doi: 10.1128/JVI.120756-12
145. De Conti L, Baralle M, Buratti E. Exon and intron definition in pre-mRNA splicing. *Wiley Interdiscip Rev RNA*. (2013) 4(1):49–60. doi: 10.1002/wrna.1140
146. Asang C, Hauber J, Schaal H. Insights into the selective activation of alternatively used splice acceptors by the human immunodeficiency virus type-1 bidirectional splicing enhancer. *Nucleic Acids Res* (2008) 36(5):1450–63. doi: 10.1093/nar/gkm1147
147. Stopak K, de Noronha C, Yonemoto W, Greene WC. HIV-1 vif blocks the antiviral activity of APOBEC3G by impairing both its translation and intracellular stability. *Mol Cell* (2003) 12(3):591–601. doi: 10.1016/S1097-2765(03)00353-8
148. Balachandran A, Ming L, Cochrane A. Chapter 6 - teetering on the edge: The critical role of RNA processing control during HIV-1 replication. In: Parent LJ, editor. *Retrovirus-cell interactions*. Academic Press (2018). p. 229–51. doi: 10.1016/b978-0-12-811185-7.00006-6
149. Bauby H, Ward CC, Hugh-White R, Swanson CM, Schulz R, Goujon C, et al. HIV-1 vpr induces widespread transcriptomic changes in CD4(+) T cells early postinfection. *mBio* (2021) 12(3):e0136921. doi: 10.1128/mBio.01369-21
150. Jordan A, Bisgrove D, Verdin E. HIV Reproducibly establishes a latent infection after acute infection of T cells in vitro. *EMBO J* (2003) 22(8):1868–77. doi: 10.1093/emboj/cdg188
151. Wu Y, Marsh JW. Selective transcription and modulation of resting T cell activity by preintegrated HIV DNA. *Science* (2001) 293(5534):1503–6. doi: 10.1126/science.1061548
152. Imam H, Bano AS, Patel P, Holla P, Jameel S. The lncRNA NRON modulates HIV-1 replication in a NFAT-dependent manner and is differentially regulated by early and late viral proteins. *Sci Rep* (2015) 5:8639. doi: 10.1038/srep08639
153. Tange TO, Jensen TH, Kjems J. *In vitro* interaction between human immunodeficiency virus type 1 rev protein and splicing factor ASF/SF2-associated protein, p32. *J Biol Chem* (1996) 271(17):10066–72. doi: 10.1074/jbc.271.17.10066
154. Truman CT, Jarvelin A, Davis I, Castello A. HIV Rev-visited. *Open Biol* (2020) 10(12):200320. doi: 10.1098/rsob.200320
155. Van Damme N, Goff D, Katsura C, Jorgenson RL, Mitchell R, Johnson MC, et al. The interferon-induced protein BST-2 restricts HIV-1 release and is downregulated from the cell surface by the viral vpr protein. *Cell Host Microbe* (2008) 3(4):245–52. doi: 10.1016/j.chom.2008.03.001
156. Kirchhoff F. Immune evasion and counteraction of restriction factors by HIV-1 and other primate lentiviruses. *Cell Host Microbe* (2010) 8(1):55–67. doi: 10.1016/j.chom.2010.06.004
157. Landi A, Iannucci V, Nuffel AV, Meuwissen P, Verhasselt B. One protein to rule them all: modulation of cell surface receptors and molecules by HIV nef. *Curr HIV Res* (2011) 9(7):496–504. doi: 10.2174/157016211798842116
158. Strebel K. HIV Accessory proteins versus host restriction factors. *Curr Opin virol* (2013) 3(6):692–9. doi: 10.1016/j.coviro.2013.08.004
159. Li X, Manley JL. Inactivation of the SR protein splicing factor ASF/SF2 results in genomic instability. *Cell* (2005) 122(3):365–78. doi: 10.1016/j.cell.2005.06.008
160. Sanford JR, Gray NK, Beckmann K, Caceres JF. A novel role for shuttling SR proteins in mRNA translation. *Genes Dev* (2004) 18(7):755–68. doi: 10.1101/gad.286404
161. Zhang Z, Krainer AR. Involvement of SR proteins in mRNA surveillance. *Mol Cell* (2004) 16(4):597–607. doi: 10.1016/j.molcel.2004.10.031
162. Aznarez I, Nomakuchi TT, Tetenbaum-Novatt J, Rahman MA, Fregoso O, Rees H, et al. Mechanism of nonsense-mediated mRNA decay stimulation by splicing factor SRSF1. *Cell Rep* (2018) 23(7):2186–98. doi: 10.1016/j.celrep.2018.04.039
163. Li X, Wang J, Manley JL. Loss of splicing factor ASF/SF2 induces G2 cell cycle arrest and apoptosis, but inhibits internucleosomal DNA fragmentation. *Genes Dev* (2005) 19(22):2705–14. doi: 10.1101/gad.1359305
164. Tazi J, Bakkour N, Marchand V, Ayadi L, Aboufirassi A, Branlant C. Alternative splicing: regulation of HIV-1 multiplication as a target for therapeutic action. *FEBS J* (2010) 277(4):867–76. doi: 10.1111/j.1742-4658.2009.07522.x
165. Bakkour N, Lin YL, Maire S, Ayadi L, Mahuteau-Betzer F, Nguyen CH, et al. Small-molecule inhibition of HIV pre-mRNA splicing as a novel antiretroviral therapy to overcome drug resistance. *PLoS pathogens* (2007) 3(10):1530–9. doi: 10.1371/journal.ppat.0030159
166. Soret J, Bakkour N, Maire S, Durand S, Zekri L, Gabut M, et al. Selective modification of alternative splicing by indole derivatives that target serine-arginine-rich protein splicing factors. *Proc Natl Acad Sci U S A* (2005) 102(24):8764–9. doi: 10.1073/pnas.0409829102
167. Soret J, Gabut M, Tazi J. SR proteins as potential targets for therapy. *Prog Mol subcellular Biol* (2006) 44:65–87. doi: 10.1007/978-3-540-34449-0\_4
168. Kemnic TR, Gulick PG. *HIV Antiretroviral therapy*. Treasure Island (FL: StatPearls (2022).



169. Pennings PS. HIV Drug resistance: Problems and perspectives. *Infect Dis Rep* (2013) 5(Suppl 1):e5. doi: 10.4081/idr.2013.s1.e5
170. Bayer F, Dremova O, Khuu MP, Mammadova K, Pontarollo G, Kiouptsi K, et al. The interplay between nutrition, innate immunity, and the commensal microbiota in adaptive intestinal morphogenesis. *Nutrients* (2021) 13(7):2198. doi: 10.3390/nu13072198
171. Sadighi Akha AA. Aging and the immune system: An overview. *J Immunol Methods* (2018) 463:21–6. doi: 10.1016/j.jim.2018.08.005
172. Shepherd R, Cheung AS, Pang K, Saffery R, Novakovic B. Sexual dimorphism in innate immunity: The role of sex hormones and epigenetics. *Front Immunol* (2020) 11:604000. doi: 10.3389/fimmu.2020.604000
173. Hasenkrug KJ, Lavender KJ, Santiago ML, Sutter K, Dittmer U. Different biological activities of specific interferon alpha subtypes. *mSphere* (2019) 4(4):e00127-19. doi: 10.1128/mSphere.00127-19
174. Lavender KJ, Pace C, Sutter K, Messer RJ, Pouncey DL, Cummins NW, et al. An advanced BLT-humanized mouse model for extended HIV-1 cure studies. *AIDS* (2018) 32(1):1–10. doi: 10.1097/QAD.0000000000001674
175. Sutter K, Lavender KJ, Messer RJ, Widera M, Williams K, Race B, et al. Concurrent administration of IFN $\alpha$ 14 and cART in TKO-BLT mice enhances suppression of HIV-1 viremia but does not eliminate the latent reservoir. *Sci Rep* (2019) 9(1):18089. doi: 10.1038/s41598-019-54650-9
176. Shirazi Y, Pitha PM. Alpha interferon inhibits early stages of the human immunodeficiency virus type 1 replication cycle. *J virol* (1992) 66(3):1321–8. doi: 10.1128/jvi.66.3.1321-1328.1992
177. Widera M, Wilhelm A, Toptan T, Raffel JM, Kowarz E, Roesmann F, et al. Generation of a sleeping beauty transposon-based cellular system for rapid and sensitive screening for compounds and cellular factors limiting SARS-CoV-2 replication. *Front Microbiol* (2021) 12(2034):701198. doi: 10.3389/fmicb.2021.701198
178. Widera M, Dirks M, Bleekmann B, Jablonka R, Daumer M, Walter H, et al. HIV-1 persistent viremia is frequently followed by episodes of low-level viremia. *Med Microbiol Immunol* (2017) 206(3):203–15. doi: 10.1007/s00430-017-0494-1
179. Phair RD, Misteli T. High mobility of proteins in the mammalian cell nucleus. *Nature* (2000) 404(6778):604–9. doi: 10.1038/35007077